Thermal Predictive Control of Electric and Hybrid Powertrain

Ammar Alaa Mohamed Shebl Ali Salem

(Matricola: 250129)

Department of Mechanical Engineering

Politecnico di Torino

A thesis submitted for the degree of

Master of Science

April 2021

Supervised by: Prof. Stefano Carabelli

ACKNOWLEDGEMENT

I am really grateful to my supervisor Prof. Stefano Carabelli for his support, guidance and for giving me this opportunity to work in this research activity.

Besides my supervisor, I would like to thank Prof. Carlo Novara for his help and recommendations.

I would also like to thank our lecturers in Politecnico di Totino whom had a hand in obtaining my degree.

Finally, I thank my family and friends for their support and inspiration.

TABLE OF CONTENTS

ACKNOWLEDGEMENT……..……. III

TABLE OF CONTENTS……...……... IV

LIST OF FIGURES..... V

LIST OF SYMBOLS……...…… VII

ABSTRACT……..…… IX

1. INTRODUCTION……...… 10
1.1 Scope and objectives……..……... 10
1.2 Thesis structure…….…… 11

2. BATTERY MODELLING……..……... 12
2.1 Electro-thermal model……..…… 12
2.1.1 Electrical model (Simple circuit model)…….… 12
2.1.2 Thermal model…… 16
2.2 Validation…….…… 18

3. BATTERY PACK DESIGN……... 22
3.1 Design of battery pack packaging box…….. 22
3.2 Thermal analysis……... 24

4. DESIGN OF EXPERIMENTS AND SIMULATION……..…… 29
4.1 Thermal dissipation of battery cells……..…… 31
4.2 Cooling system…….…… 33
4.2.1 Ambient air cooling……. 33
4.2.2 Cooled air cooling……... 35

5. PREDICTION AND DERATION…….…… 36
5.1 Motor prediction……...……. 37
5.2 Battery prediction…….…… 37
5.3 Prediction Accuracy…….…. 39
5.3.1 Prediction horizon length……..... 39
5.3.2 Time history length……..... 43
5.4 Deration…….…… 44
5.4.1 Studied de-rate strategies…….…… 44
5.4.2 Implementation……...……. 46
5.4.3 No cooling……... 46
5.4.4 Ambient air cooling……..……... 52

6. CONCLUSION……..…… 58

REFERENCES…….……. 59

LIST OF FIGURES

Figure 2.1: battery equivalent circuit model……..…….13
Figure 2.2: Datasheet battery block……..……14
Figure 2.3: capacity at various discharge currents for LG cell……..…….14
Figure 2.4: SOC and voltage level at different currents for LG cell……..…..15
Figure 2.5: OCV as a function of SOC for LG cell……..……15
Figure 2.6: Thermal model equivalent circuit……..…17
Figure 2.7: Battery module inside climatic chamber……..…….19
Figure 2.8: 1st test: battery voltage and current. 1: experiment, 2: simulation…….……20
Figure 2.9: 1st test: battery temperature. 1: experiment, 2: simulation…….20
Figure 2.10: 2nd test: battery voltage and current. 1: experiment, 2: simulation……..21
Figure 2.11: 2nd test: battery temperature. 1: experiment, 2: simulation…….…….21
Figure 3.1: Simulink model – Comparison between LG and Samsung cells…….…..22
Figure 3.2: The shape of battery pack……..22
Figure 3.3: Battery pack packaging box design……...…23
Figure 3.4: Vertical cross section in battery packaging box……...….24
Figure 3.5: Fin illustrative drawing……..……24
Figure 3.6: Heat transfer equivalent circuit……..25
Figure 4.1: Driving cycle…….……29
Figure 4.2: Average heat generation of LG and Samsung battery cells…….…….31
Figure 4.3: Maximum temperature of LG and Samsung battery cells…….……31
Figure 4.4: Battery overheat duration…….…..32
Figure 4.5: Average cooling power and average battery heat generation – ambient air……..33
Figure 4.6: Maximum battery temperatures – ambient air…….……..34
Figure 4.7: Battery overheat duration for every condition – ambient air…….....34
Figure 4.8: Average cooling power and average battery heat generation – Cooled air…...…35
Figure 4.9: Maximum and average battery temperatures – Cooled air……..…..35
Figure 5.1: MATLAB Simulink prediction function……..…… 36
Figure 5.2: Example of prediction……38
Figure 5.3: Step response of battery thermal dynamics…….. 39

Figure 5.4: Step response of motor thermal dynamics…….... 40
Figure 5.5: Temperature prediction error of 180 seconds prediction horizon……. 41
Figure 5.6: Temperature prediction error for 300 seconds prediction horizon……...… 41
Figure 5.7: Temperature prediction error for 600 seconds prediction horizon……...…… 42
Figure 5.8: Temperature prediction error for 180 seconds time history length…….. 43
Figure 5.9: Example of deration – road slope 10%, ambient temperature 25 °C…….…... 45
Figure 5.10: Torque rate limiter between driver's command and motor……..….. 46
Figure 5.11: Torque rate limiter…….……. 46
Figure 5.12: Average battery heat generation – no cooling…… 47
Figure 5.13: Maximum battery temperatures – no cooling……..……...…… 47
Figure 5.14: Battery overheating duration – no cooling…….…… 48
Figure 5.15: Specific consumption with regeneration – no cooling……...… 48
Figure 5.16: Battery final SOC – no cooling……....…. 49
Figure 5.17: Maximum motor temperature – water cooled……. 49
Figure 5.18: Error in battery temperature prediction……..… 50
Figure 5.19: Velocity profile error – no cooling……..…...… 51
Figure 5.20: Average battery heat generation – ambient air cooling……..…… 52
Figure 5.21: Cooling power – ambient air cooling……..…...… 52
Figure 5.22: Maximum battery temperature – ambient air cooling……...…. 53
Figure 5.23: Battery overheating duration – ambient air cooling……..……. 53
Figure 5.24: Specific consumption with regeneration – ambient air cooling……..….... 54
Figure 5.25: Battery final SOC – ambient air cooling……...……. 54
Figure 5.26: Battery temperature prediction error – ambient air cooling……...…… 55
Figure 5.27: Velocity profile error – ambient air cooling……...… 55
Figure 5.28: Driving modes duration – no cooling…….…… 57
Figure 5.29: Driving modes duration – ambient air cooling……..……. 57

LIST OF SYMBOLS

Symbol	Meaning
OCV	Open Circuit Voltage
R_i	Battery internal resistance
V_T	Battery terminals voltage
I_b	Battery current
Q_{nom}	Battery nominal capacity
SOC	State of Charge
T_b	Uniform battery temperature
Q_b	Generated thermal power inside the battery
m_b	Battery mass
$C_{p,b}$	Battery Specific heat
Q_{loss}	Heat transfer rate to the surrounding
l_f	Fin length (tube height)
t_f	Fin thickness
w_f	Fin width
w_{tube}	Tube width
l_{tube}	Tube length
t_{bottom}	Box base thickness
A_{bottom}	Total box bottom surface area
A_{tubes}	Inner surface area of tubes upper surface
$R_{contact}$	Thermal contact resistance between battery and box base
R_{cond}	Thermal conduction resistance through box base
R_{base}	Thermal convection resistance from tube inner top area
$R_{f,N}$	Fins thermal resistance
q_f	Heat transfer rate through fin
p	Fin perimeter
A_c	Fin cross-sectional area
N_f	Number of fins
T_∞	Coolant inlet temperature

k_{box}	Box material conductive heat transfer coefficient
h	Convective heat transfer coefficient
k_c	Thermal conductivity of the cooling fluid
D_h	Tube hydraulic diameter
Nu	Nusselt number
Re	Reynolds number
u	Cooling fluid inlet velocity
ν	Kinematic viscosity of cooling fluid
Pr	Prandtl number
Q_{cool}	Heat transfer rate from battery pack to the cooling fluid
C_b	Battery thermal capacity
BMS	Battery Management System
T_{amb}	Ambient temperature
Q_m	Motor heat generation rate
T_m	Motor temperature
T_c	Motor coolant temperature
R_{mc}	Thermal resistance between motor and coolant
C_m	Motor thermal capacity
C_c	Motor coolant thermal capacity
k_r	Radiator thermal transfer coefficient
A_r	Radiator frontal area
R_{ba}	Thermal resistance between battery and air

ABSTRACT

In the modern era of electric vehicles battery design and management is of a significant importance for electric vehicles performance and development. Specifically, thermal management of battery pack since overheating is a main issue for cooling system design. In this thesis, a model-based design approach is used to design a battery pack as well as the cooling system regardless of cell type. In addition, model accuracy has been proved through an experiment performed using a module composed of 10 Samsung 94Ah cells in series. MATLAB Simulink has been used as a tool for performing analysis and calculations. Comparison was held between two different cells and the one with better thermal behaviour is selected. Furthermore, a battery management strategy implementing a more complicated control algorithm based on prediction of the future battery temperature is applied to avoid battery overheating in extreme situations by applying necessary changes in the inverter.

1. INTRODUCTION

Electric vehicles (EVs) have emerged as a new promising means of transportation which is clean and emission-free [1]. Conventional vehicles using internal combustion engines are major source of CO_2 emissions [2]. With generating higher amounts of electricity from renewable energy EVs are being promoted by many countries to replace conventional vehicles that caused pollution and energy problems [2]–[4]. In 2019, the number of EVs in market reached 7.2 million vehicle with 40% increase with respect to past year and Europe was the biggest market after China. According to countries policies towards EVs it is expected in 2030 that EVs sales will reach 140 million vehicles that is about 7% of total market. This in turn could save about 2.5 million oil barrels per day [2]. Yet some challenges face EVs especially pure electric vehicles mainly, they are covered range by one charge, battery charging time and battery management. Hence, battery is an extremely important part that heavily impact vehicle performance and has a big influence on EVs development. Unlike conventional vehicles, an electric vehicle draws energy continuously from the battery as the main power source so there is the need of high capacity e.g. high specific energy and high specific power[5], [6]. Many types of batteries have been introduced and lithium-ion batteries are the best to meet the requirements of EVs as they have high energy density and high specific energy as well as cycle life [2], [7]–[9].

1.1 Scope and objectives

In this thesis, work is focused on the battery design and management. A major problem that faces EVs is battery overheating. This issue affects vehicle performance significantly, high temperature variations decreases battery life [10] also, if battery temperature rises close to its maximum safety threshold the inverter limits maximum motor torque to low value, which in turn limits vehicle ability. Thus, an efficient thermal management system is of crucial importance along with a battery cell with good thermal characteristics and low internal resistance. The main goal of this thesis project is using model-based design approach to design a 10 kWh battery pack choosing from different alternatives of Lithium-ion cells based on their thermal behavior then developing a thermal management system depending on battery temperature prediction. Firstly, a Simulink electro-thermal model is developed regardless of cell type. Using Simulink model, a comparison is held between cells to investigate their thermal behavior without any cooling or control. In parallel to the modelling, results of an experiment have been utilized for model validation to show that the model has a high accuracy. After that, the selected cell is used for making the required battery as well as a cooling system utilizing ambient air or cooled air is designed and applied. Finally, a de-rate strategy implementing a control algorithm depending on the prediction of future temperature of the battery based on the current circumstances is applied to avoid battery overheating (below 55^{o}C for chosen cell). Unlike conventional de-rate strategy that is already present in an inverter that depends on the current temperature of the battery and it limits the maximum torque of the motor which limits the vehicle ability in some situations. The de-rate strategy developed in this thesis takes action based on future state prediction before it actually happens and this strategy limits the rate of motor torque increase so the vehicle could still keep its ability but at a slower rate of response in extreme situations.

1.2 Thesis structure

Chapter 1: Introduction, scope and objectives.

Chapter 2: Battery electro-thermal model is developed on MATLAB Simulink and model validation is presented.

Chapter 3: Battery pack design along with cooling system design and analysis are described.

Chapter 4: Contains simulation and experiment design. Some realistic situations of road slope and temperatures that the vehicle might face are reported. Also, the comparison between the two proposed cells (LG cylindrical cells Vs. Samsung prismatic cells) is performed.

Chapter 5: Prediction algorithm of future battery temperatures is described and the de-rate strategy based on that prediction.

Chapter 6: Conclusion.

2. BATTERY MODELLING

In literature, numerous battery models have been reported. Models vary in terms of complexity, accuracy and needed computational power. The choice is made based on the required information that to be reported from the model amd a trade-off between complexity and accuracy. Studied models are:

Electro-chemical model [11]–[13]:

Electro-chemical model is a very accurate model capable of capturing all cell dynamics. Whereas this model is represented by a complicated partial differential algebraic equations and it needs a huge computational power. Also, it depends on enormous number of parameters, which depend on cell chemistry and geometry. Therefore, this model is not suitable for real time applications from a practical point of view.

Reduced order electrochemical model [14]:

Some simplification have been made to the previous model to make it easier for implementation but with sacrificing some accuracy. Parameters required for this model can be obtained by measuring battery signals.

Equivalent circuit model [15]–[18]:

A simplified model contains simple electric elements e.g. resistors and capacitors. A circuit composed of these components models the battery behaviour. Advantages of this model are: Simplicity, easiness of parametrization, low number of parameters needed and less computational time. In addition, this model has a relatively high accuracy besides its simplicity. These advantages make it more suitable for real-time applications. The simplest form of this model is simple circuit model with zero time constant shown in figure 2.1. This last model is to be used when battery dynamic behaviour is not of interest.

2.1 Electro-thermal model

2.1.1 Electric model:

Simple circuit model with zero-time constant is the chosen model in this thesis. The accuracy of this model has been proved experimentally as reported in the validation section at the end of this chapter. This model can be parametrized easily with different battery cells so, it can be called modular. Also, it is often coupled with a thermal model to predict the overall battery activity. In this model Open Circuit Voltage (OCV) is directly related to State of Charge (SOC). Battery terminals voltage is given by the following equation:

$$V_T = OCV - I_b R_i$$

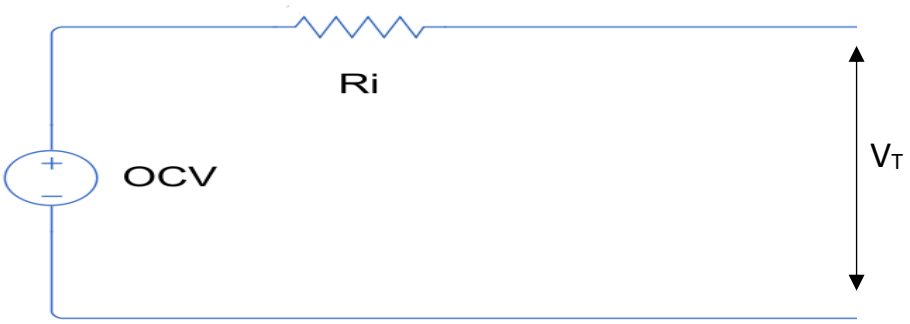

Figure 2.1: Battery equivalent circuit model.

Where:

R_i – Battery internal resistance [Ω].

OCV – Open circuit voltage [V].

V_T – Battery terminals voltage [V].

I_b – Battery current [A].

For building this model in Simulink environment "Datasheet battery" block is used figure 2.2. This block requires the definition of battery cell parameters which are:

- Nominal capacity [Ah].
- Open circuit voltages [V].
- Internal resistances [Ω].
- Battery temperature break points.
- Number of cells in parallel and number of cells in series.

These parameters are obtained from battery cell datasheet.

These are the implemented equations by datasheet battery block:

$$V_T(SOC, T_b) = OCV(SOC) - I_b R_i(SOC, T_b)$$

$$SOC = \frac{1}{Q_{nom}} \int_0^t I_b \, dt$$

Where:

Q_{nom} – Battery nominal capacity [Ah].

SOC- Battery state of charge.

T_b – Uniform battery temperature [K].

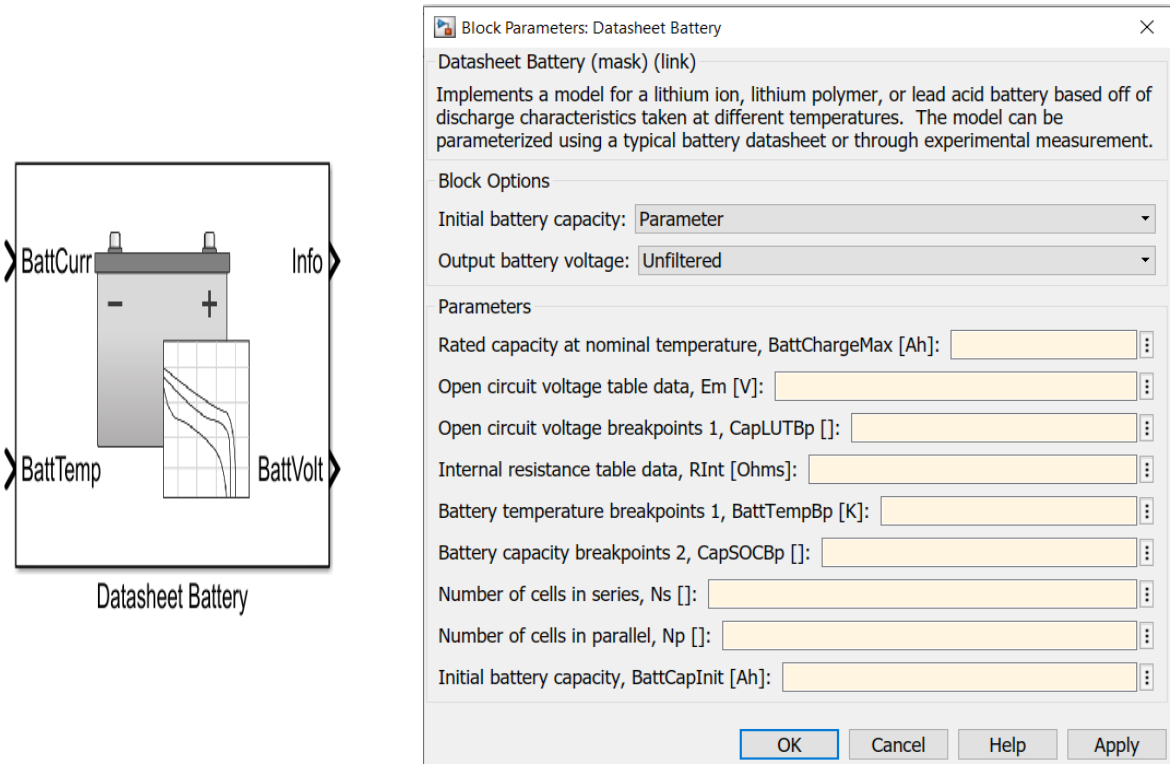

Figure 2.2: Datasheet battery block

- **Parameters definition for the electrical model:**

Battery datasheet contains plots representing discharge characteristics at different currents and different temperatures, an example shown in figure 2.3. These plots can be used after some manipulations to extract and define the parameters of battery cell needed for Datasheet battery block.

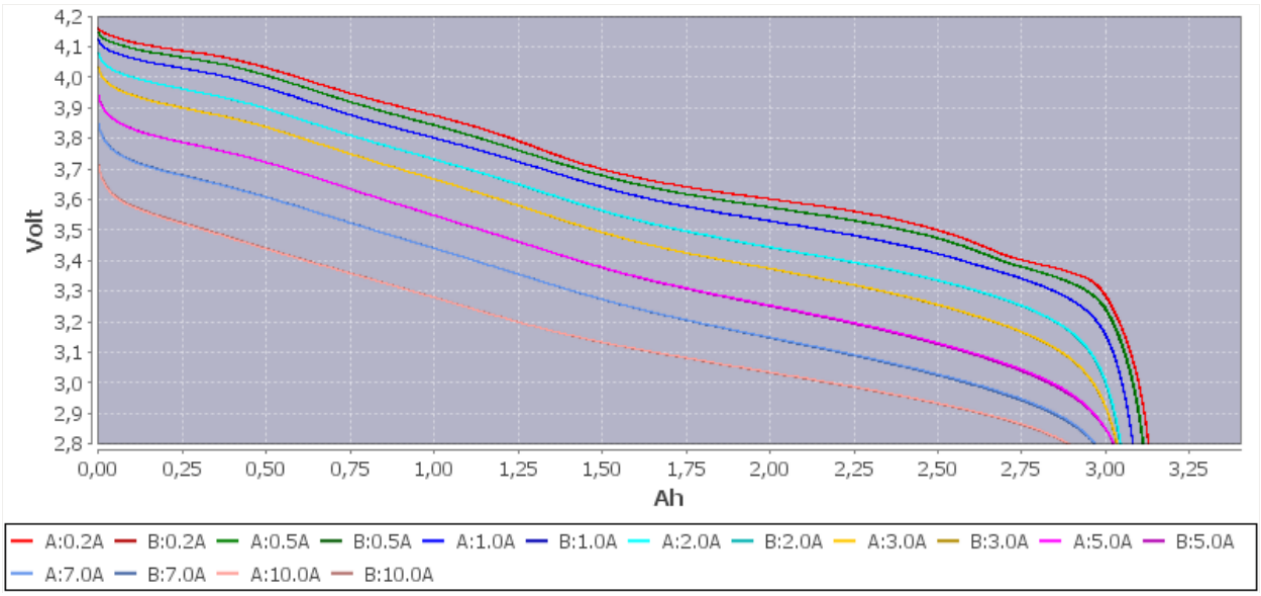

Figure 2.3: capacity at various discharge currents for LG cell.

These curves are imported and stored in MATLAB in the form of matrices. Next step is to divide each curve into segments from its maximum point to its minimum point. Then record battery voltage and state of charge (SOC) at each point, to have the levels of SOC and voltage values at each current, figure 2.4.

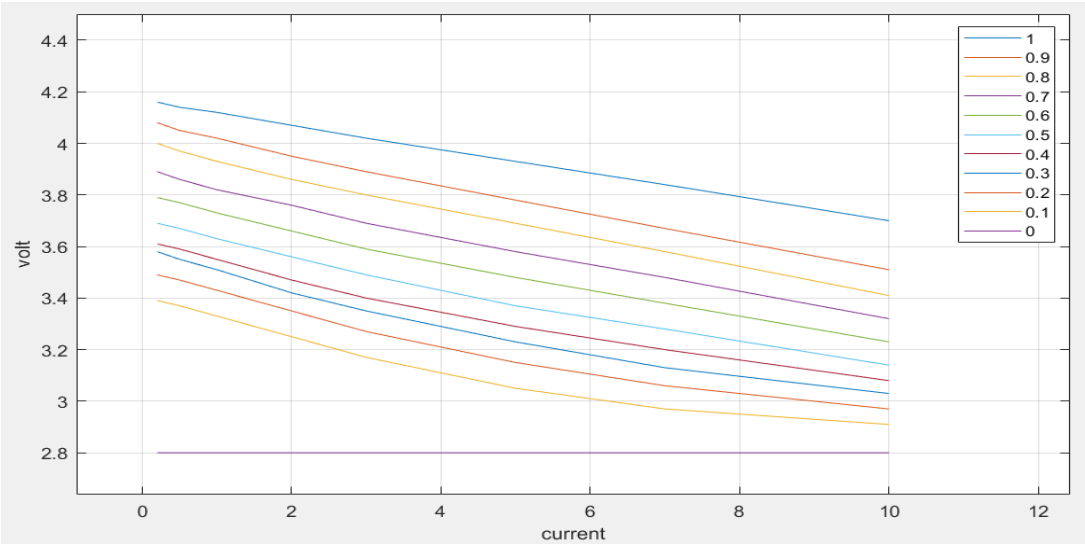

Figure 2.4: SOC and voltage level at different currents for LG cell.

A mathematical relation was found between voltage and current at different SOC values. By extrapolating each curve in figure 2.4 to zero current the open circuit voltage (OCV) as a function of SOC was found, figure 2.5.

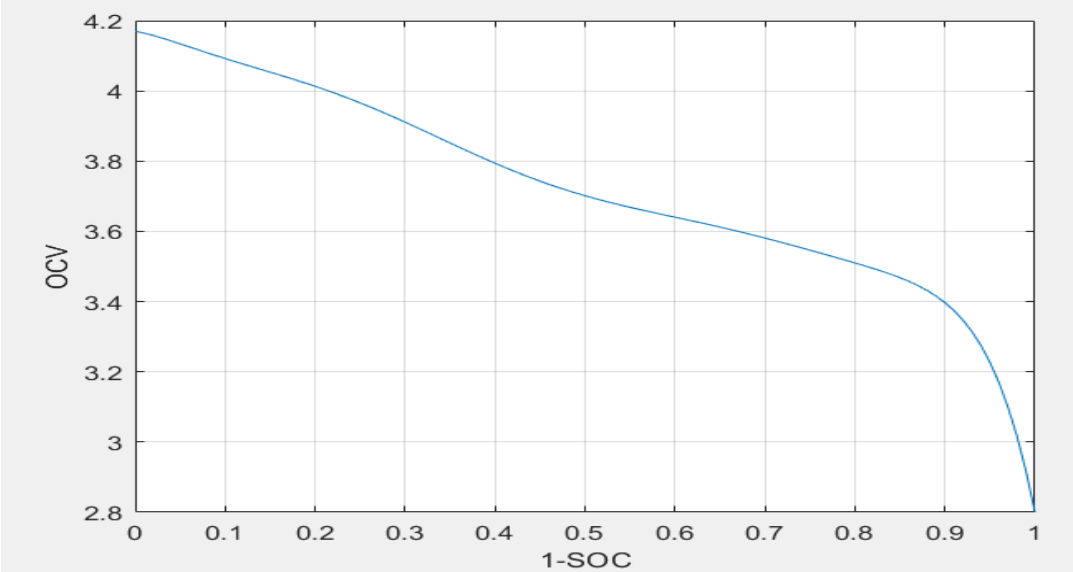

Figure 2.5: OCV as a function of SOC for LG cell.

- **Internal resistance:**

Battery internal resistance accounts for the voltage drop inside the battery when connected to a load compared to no-load condition. Internal resistance depends on the SOC, temperature, chemical properties of the battery and aging. In this thesis it is considered as a function of SOC and battery temperature according to the following equation:

$$R_i(SOC, T_b) = \frac{OCV(SOC) - V_T(SOC, T_b)}{I_b}$$

For every test temperature the internal resistance was calculated for every SOC breakpoint then the internal resistance is obtained and tabulated as a function of temperature and SOC. The parameters reported above are imported into the datasheet battery block in Simulink.

2.1.2 Thermal model:

During battery charging and discharging battery temperature increases so, it is necessary to have a proper thermal model coupled with the electrical model to simulate the whole behaviour of the battery especially battery temperature parameter is required as an input to the Datasheet battery block.

Heat generation inside battery cell is due to electrical heating called Joule heating effect. Voltage drop during discharge in cell inter resistance (Or increase during charge) corresponds to an irreversible transformation of electrical energy into heat.

The amount of heat generation rate is given by:

$$Q_b = I_b * (OCV - V_T)$$

Or

$$Q_b = I_b^2 R_i(SOC, T_b)$$

Energy balance of a battery cell is as follows:

$$Q_b = I_b^2 R_i(SOC, T_b) = m_b C_{p,b} \frac{dT_b}{dt} + Q_{loss}$$

Where:

Q_b: Generated thermal power inside the battery [W].

m_b: Battery mass [kg].

$C_{p,b}$: Battery Specific heat [J/kg.K].

Q_{loss}: Heat transfer rate to the surrounding [W].

The following equivalent circuit in figure 2.6 can show this.

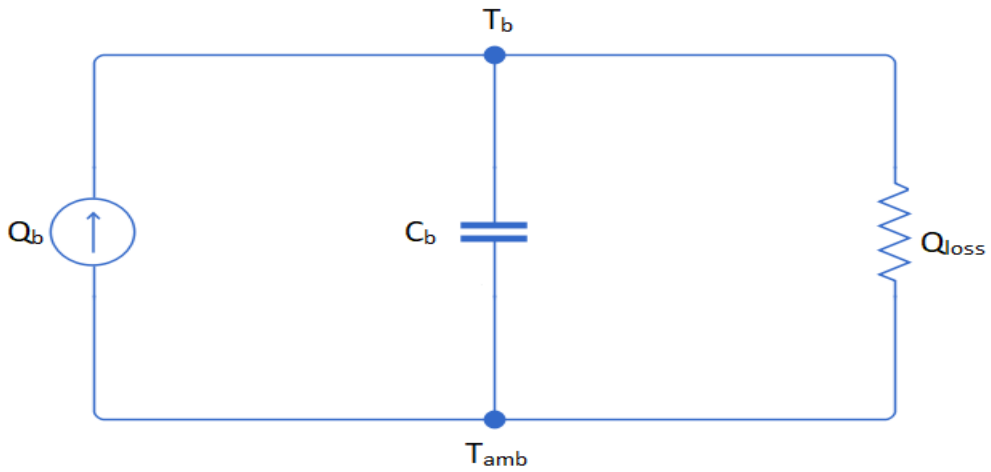

Figure 2.6: Thermal model equivalent circuit.

$\boldsymbol{m_b C_{p,b} \frac{dT_b}{dt}}$**:** Represents the part of heating power stored inside the battery and causes temperature increase, so it is a storage term. Shown by the capacitor.

$\boldsymbol{Q_{loss}}$**:** Represents the part of heating power transferred out of the battery and lost either naturally to the surrounding or absorbed by a cooling system. Also, it can be zero if the battery does not exchange heat with another medium which means all generated power participated in elevating battery temperature. Because it is a loss term it is shown by the resistor.

2.2 Model validation

In this section, the reliability of the aforementioned battery model is tested experimentally to verify its accuracy in representing the real behavior of the battery. The following experiment is performed and its results are represented below.

Samsung-94Ah cell is used to make a battery module consists of 10 cells connected in series, table 2.1, and its parameters were imported into MATLAB Simulink model. A test bench is constructed in a climatic chamber and all tests were performed inside the chamber at temperature of 25 ºC without cooling system except for the natural convection with the surrounding air this is shown in figure 2.7.

		Element	Module
Nominal voltage	*V*	**3,7**	**37**
Upper limit voltage	*V*	*4,15*	*41,5*
Lower limit voltage	*V*	*2,7*	*27*
Nominal capacity	*Ah*	**94**	**94**
Specific capacity	*Ah/kg*	46	3
Nominal energy	*kWh*	**0,35**	**3,48**
Specific energy	*Wh/kg*	168,83	126,01
Continuous discharge current	*A*	**188**	**188**
Continuous discharge power	*kW*	0,70	6,96
Specific discharge power	*W/kg*	337,67	252,03
Max discharge current (5 s)	*A*	**282**	**282**
Max discharge power	*kW*	1,04	10,43
Continuous charge current	*A*	**47**	**47**
Continuous charge power	*kW*	0,17	1,74
Max charge current (5 s)	*A*	**188**	**188**
Max charge power	*kW*	0,70	6,96
Life cycle	#	4000	
Curb weight	*kg*	2,06	20,6
Structure weight	*kg*	0	7
Total weight	*kg*	**2,06**	**27,6**
Height	*mm*	125	175
Width	*mm*	173	201
Thickness	*mm*	45	486
Volume	*l*	**0,97**	**17,10**
Series	---	90	10
Parallel	---	1	1

Note	---	**All values @25 °C AND SoC 50%**

Table 2.1: Samsung-94Ah cell and module characteristics.

Experiment is performed several times charging and discharging the battery at different currents values and battery temperature is measured. The same tests conditions were reproduced virtually in MATLAB Simulink and battery temperature is obtained analytically as well. Then the real curve and virtual curve are compared.

It is evident from the results below that this model can represent the real behavior of the Lithium-ion battery. This model has been used to design a battery pack and run various simulation tests to predict the behavior of the battery in different situations

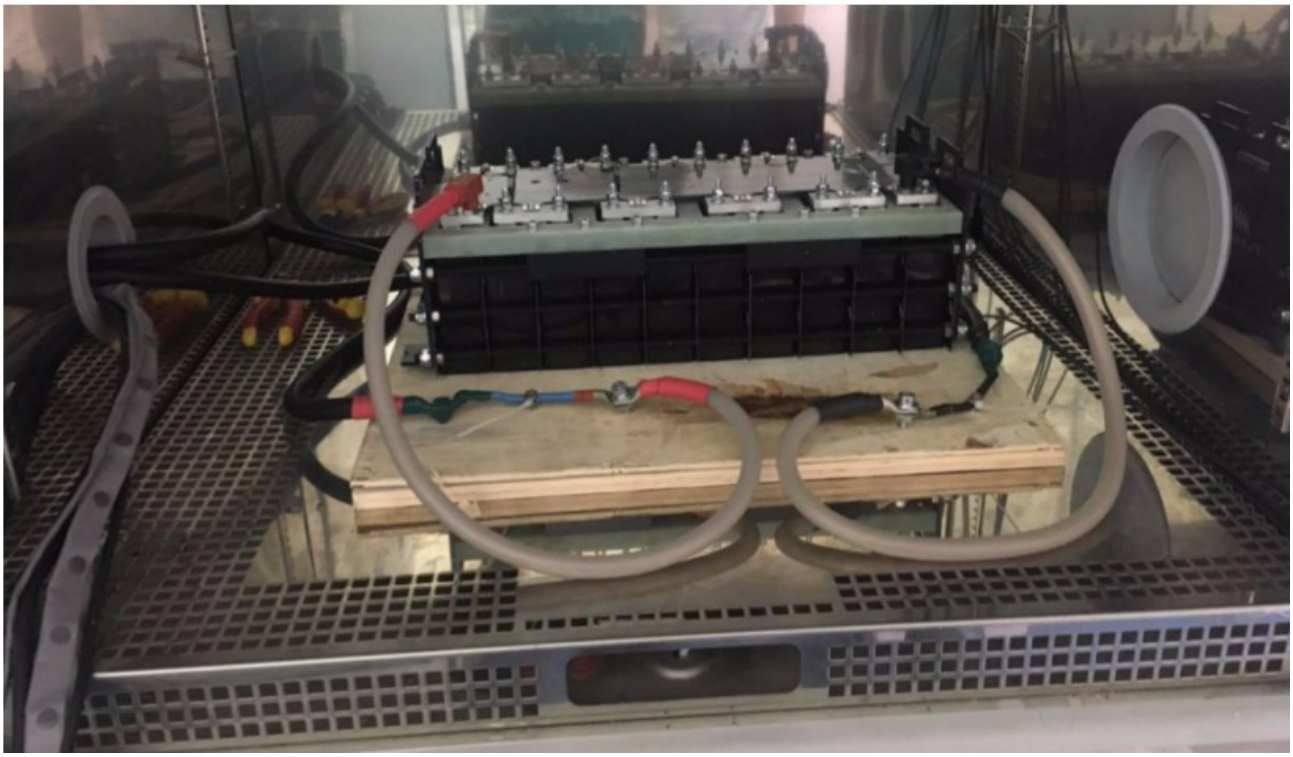

Figure 2.7: Battery module inside climatic chamber.

.

1st test: full rated ½ C charge and 1C, 1.5C discharge

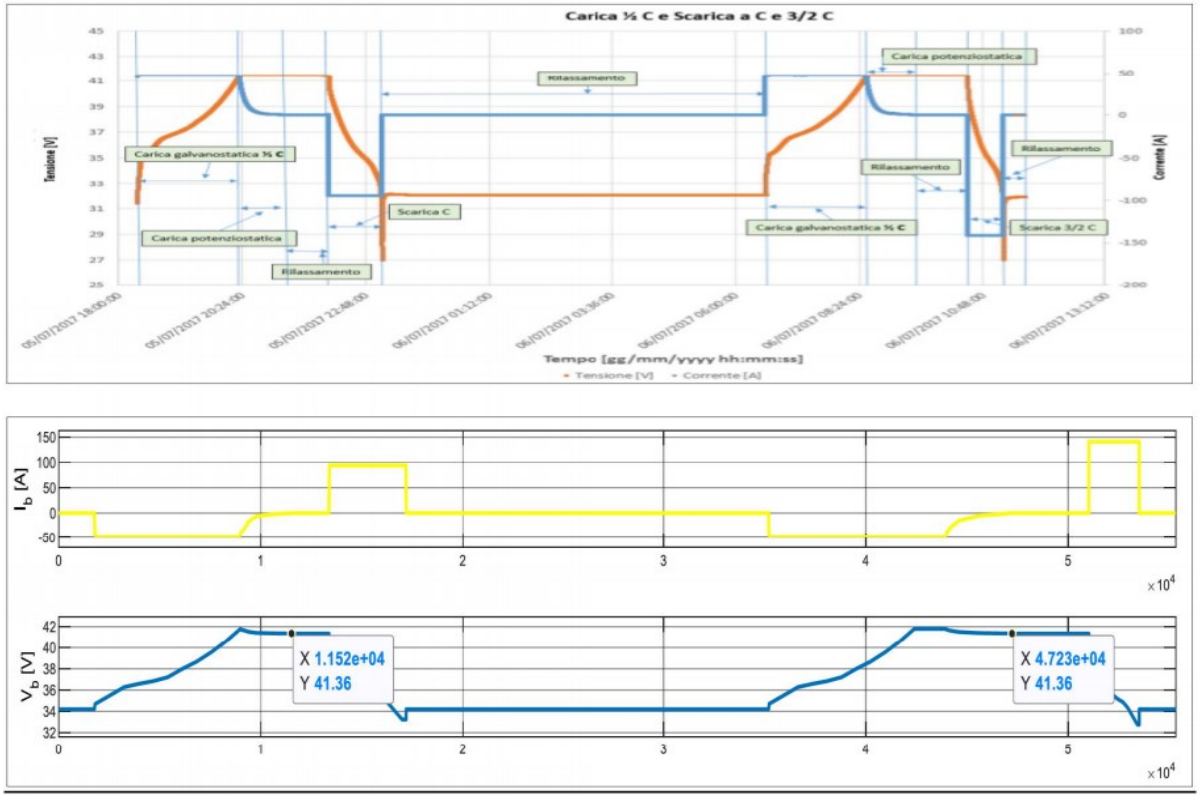

Figure 2.8: 1st test: battery voltage and current. 1: experiment, 2: simulation.

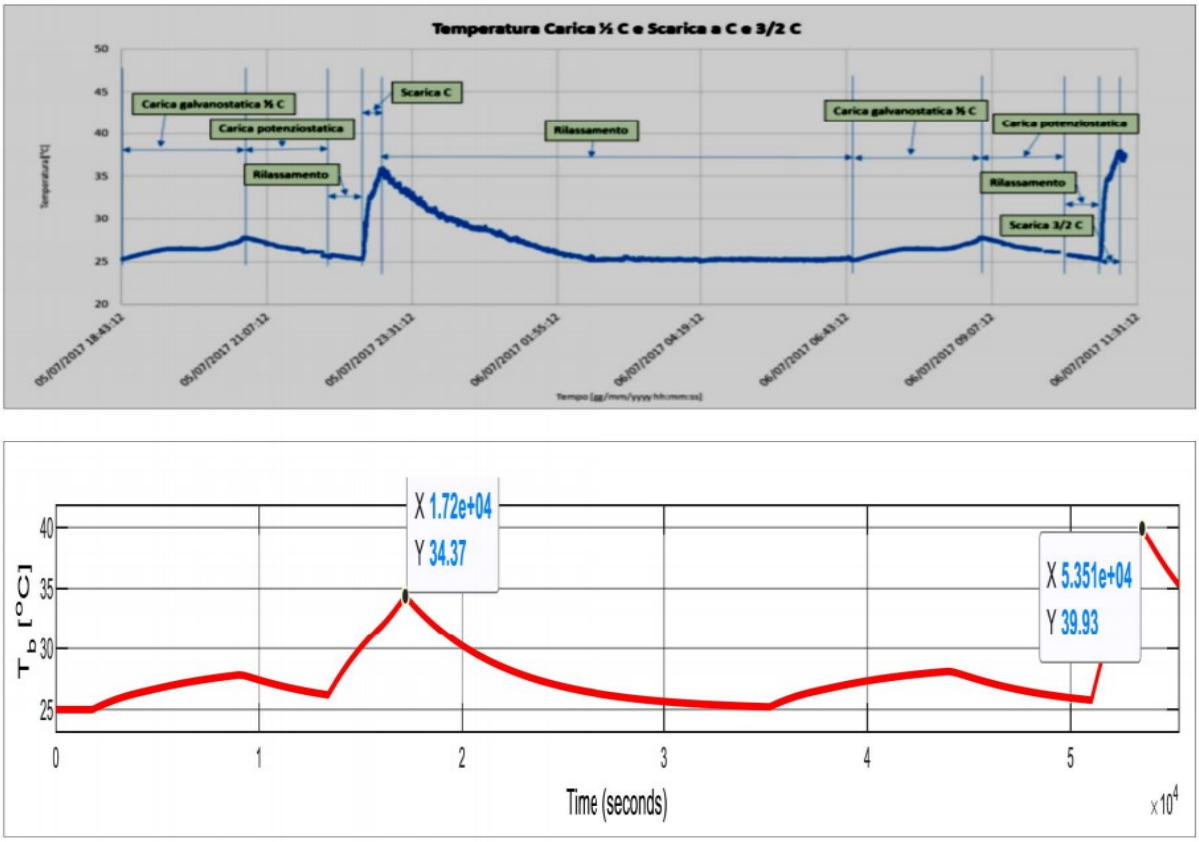

Figure 2.9: 1st test: battery temperature. 1: experiment, 2: simulation.

2nd test: full rated ½ C charge and impulse train 1C discharge

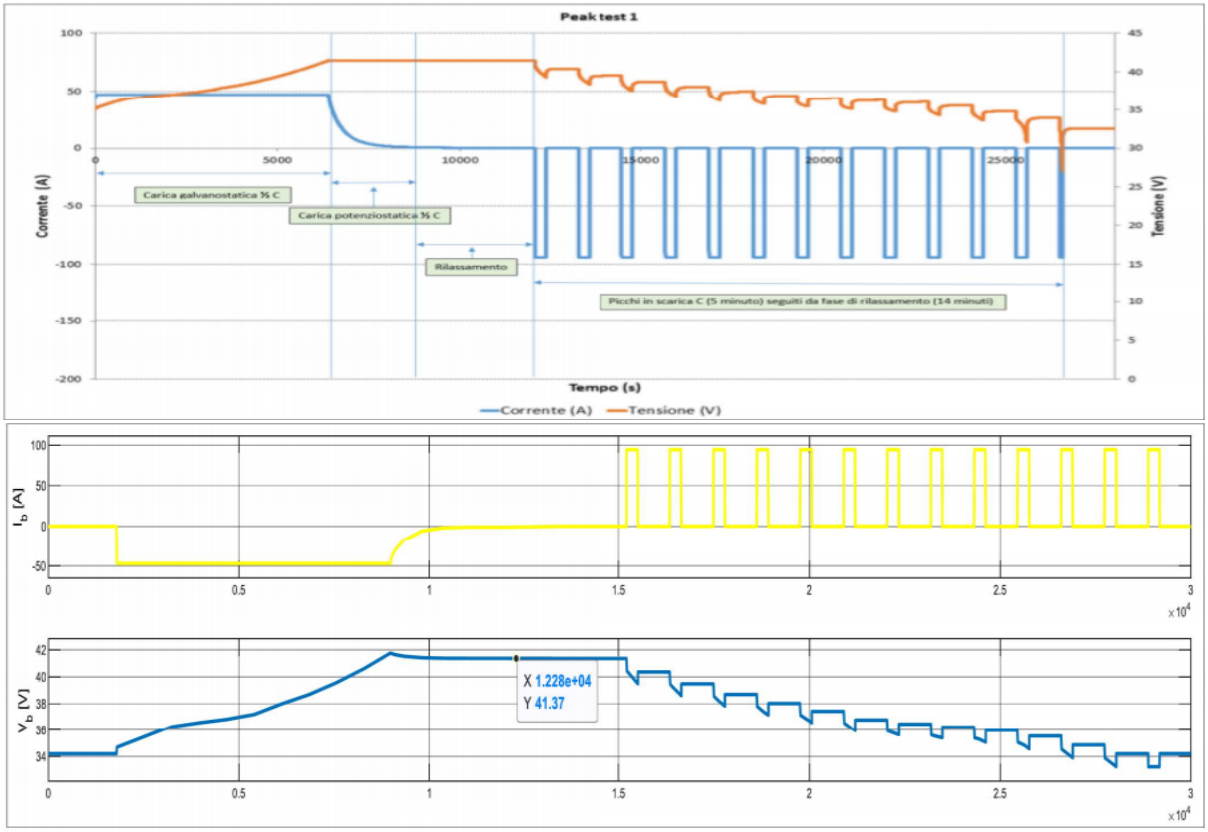

Figure 2.10: 2nd test: battery voltage and current. 1: experiment, 2: simulation.

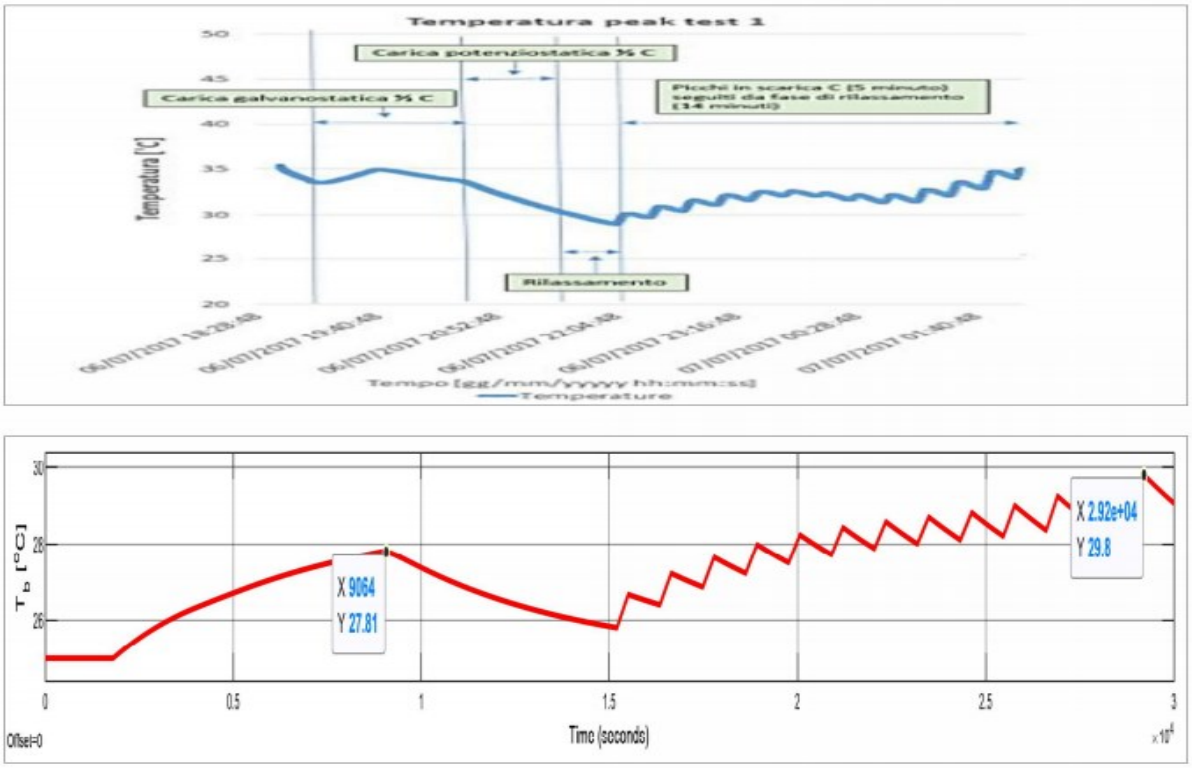

Figure 2.11: 2nd test: battery temperature. 1: experiment, 2: simulation.

3. BATTERY PACK DESIGN

This chapter represents the design process of the battery pack. The main goal is to design a 10 kWh battery pack. There are two different cells available: LG cylindrical cell and Samsung prismatic cell. They differ in their characteristics as reported below. As stated earlier battery overheating is a crucial issue so the choice is based on thermal characteristics of the two cells. This comparison is easily conducted using the developed modular MATLAB Simulink model by only changing the parameters in the script file.

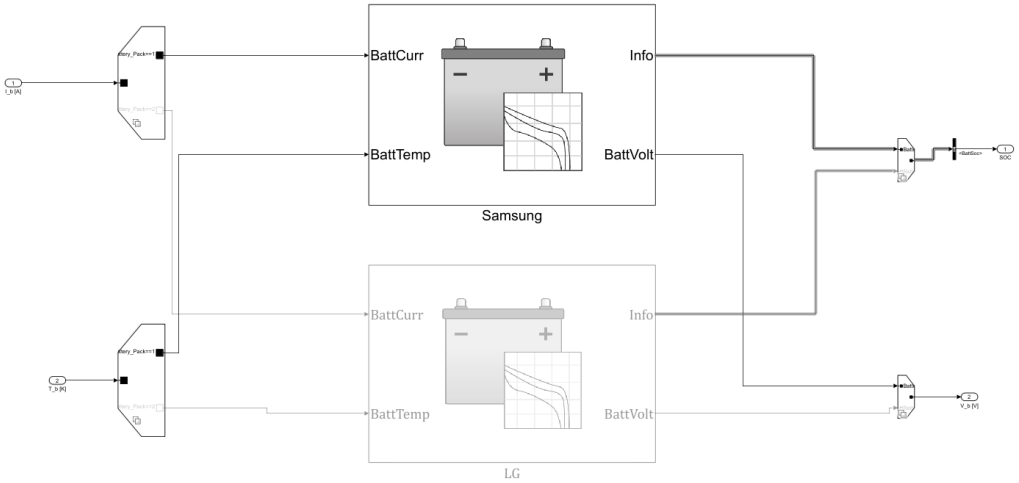

Figure 3.1: Simulink model – Comparison between LG and Samsung cells.

After choosing the best battery cell different designs of cooling systems will be studied to see which one is better for the chosen battery pack. Two proposed solutions are cooling by ambient air forced by vehicle speed with auxiliary fan at very low speeds and cooling by cooled air in a very hot weather.

3.1 Design of battery pack packaging box

Shape and dimensions of the battery pack are already specified based on packaging constraints under the vehicle, figure 3.2.

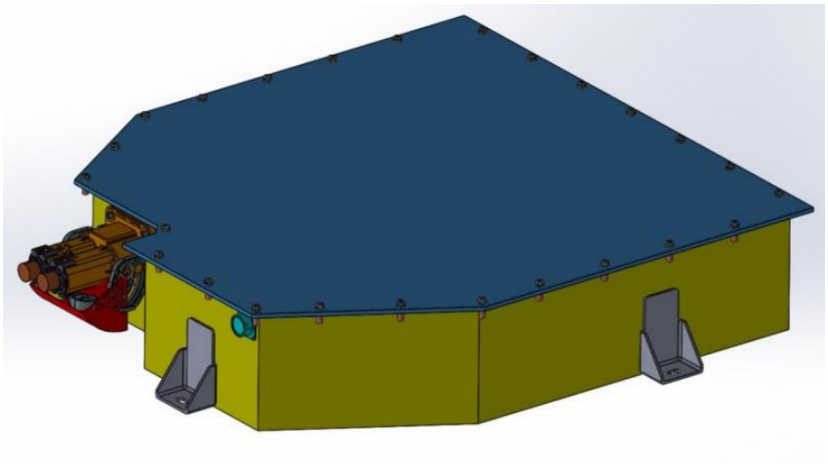

Figure 3.2: The shape of battery pack.

- **Samsung (prismatic) vs. LG (cylindrical) cells**

The following table shows the specifications of each battery cell and total number of cells to form the required battery:

Characteristics	LG	Samsung
Cell volume [l]	0.02	0.375
Cell mass [kg]	44.5	875
Number of cells in parallel	30	2
Number of cells in series	28	28
Nominal capacity [Ah]	3.2	50
Overheat limit temperature [^{0}C]	40	55

Table 3.1: Specifications of LG and Samsung cells.

Thermal behavior is the main difference that is to be studied which depends mainly on cell internal resistance. Discharging or charging the battery increases its temperature. High temperature increases reaction rate and generates even higher temperatures. Unless heat is rejected from the battery faster that it is generated a thermal run away will finally occur. Also, there is a maximum safe limit of the temperature that the battery can reach for safe use otherwise a safety shutdown is forced by Battery Management System (BMS). Even at temperatures very close to the safety threshold motor torque is limit to low values to limit discharge current, which in turn limits the rate of heat generation inside the battery.

Battery pack is enclosed in a box reinforced at the bottom by tubes for carrying the cooling fluid as shown in figure 3.3. This design allows using no cooling, ambient air cooling, cooled air cooling or even water cooling by just modifying the parameters in Simulink model.

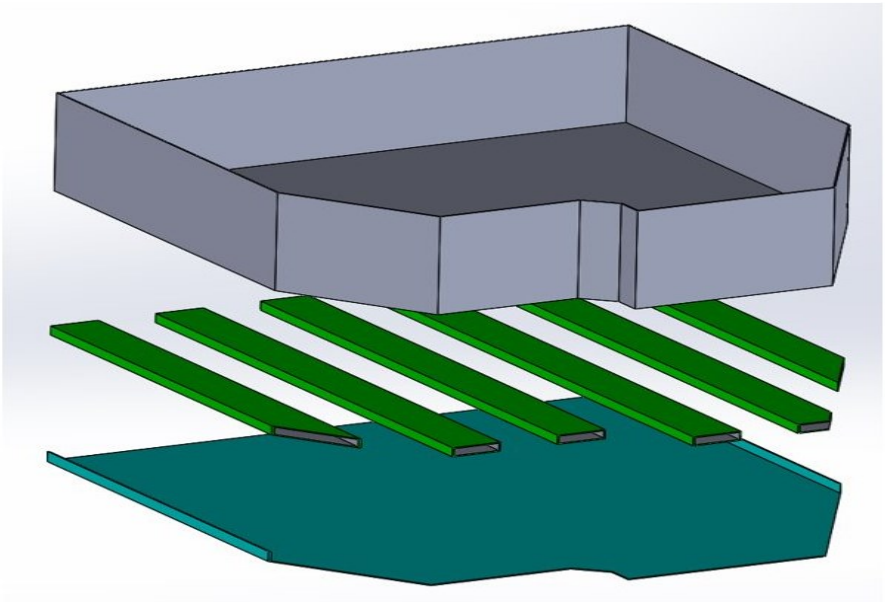

Figure 3.3: Battery pack packaging box design.

3.2 Thermal analysis

Battery cells are in direct contact with the base of the box and heat is transferred from a cell base to box base then to the coolant through the following mechanisms mentioned next, also shown in figure 3.4. Sidewalls of the tubes in the bottom of the box base are considered as fins, figure 3.5 shows an illustrative drawing of a fin.

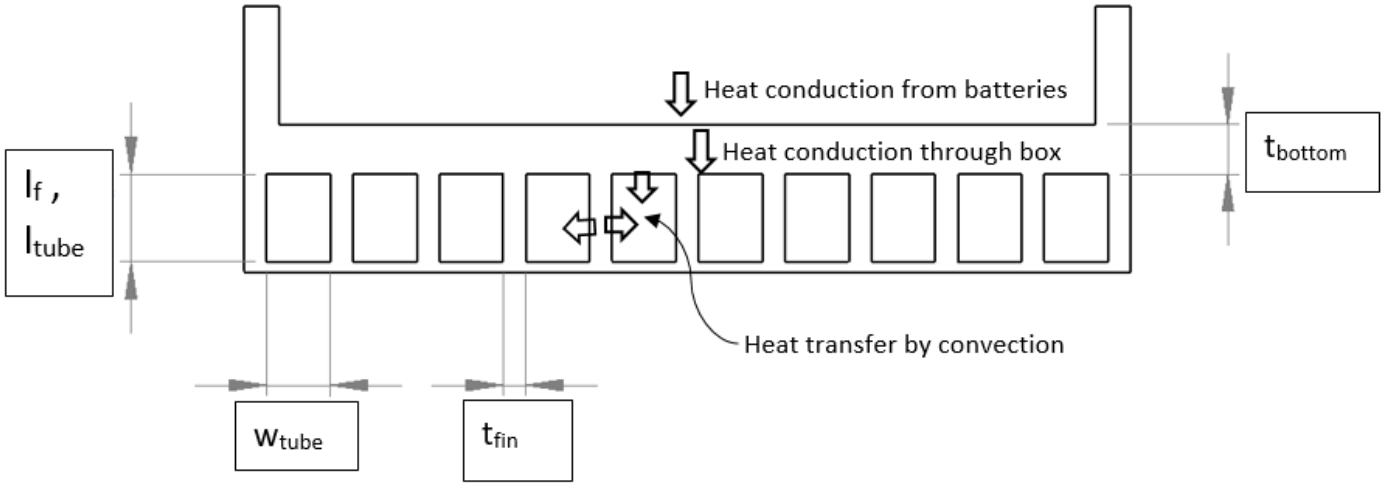

Figure 3.4: Vertical cross section in battery packaging box.

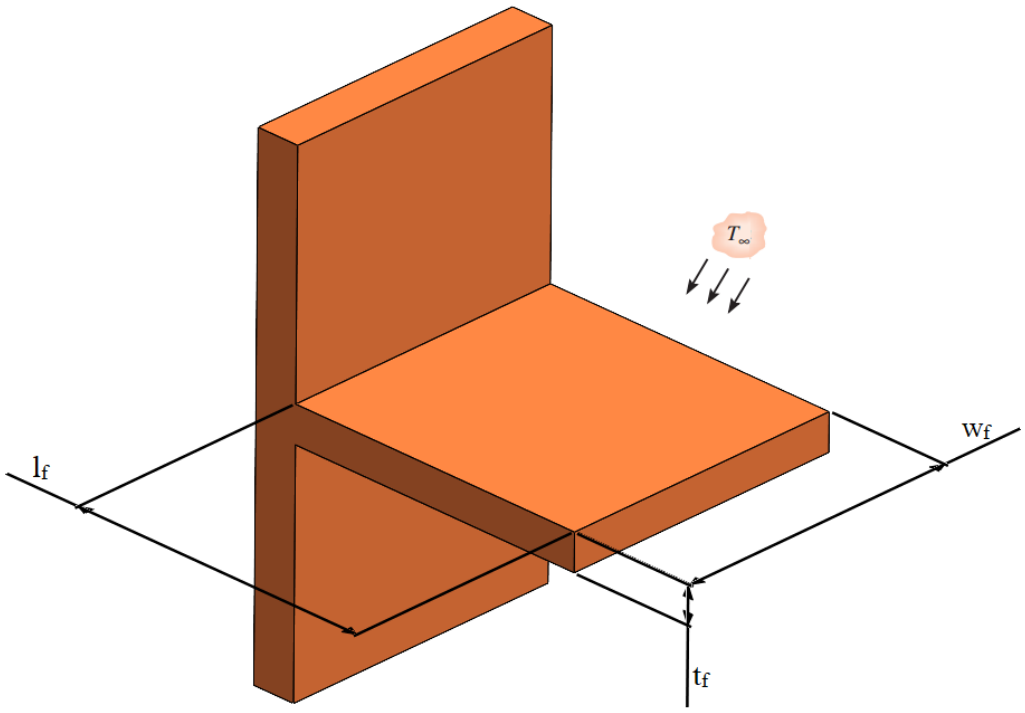

Figure 3.5: Fin illustrative drawing.

Heat transfer mechanisms from battery pack to the coolant:

- By conduction from battery to the box base.
- By conduction through box base material.
- By conduction from box base to the tubes sidewalls (considered as fins).
- By convection to the coolant through the tubes top inner surface area.
- By convection to the coolant through the tubes side walls (considered as fins).

Figure 3.6 below shows the equivalent circuit:

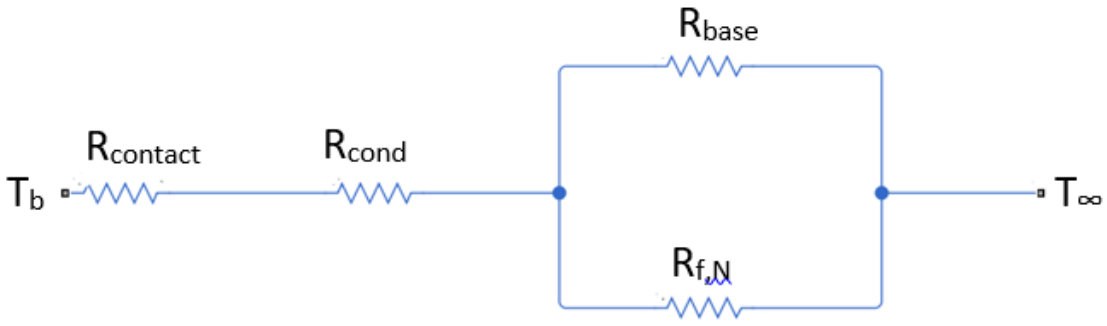

Figure 3.6: Heat transfer equivalent circuit.

Analysis:

The thermal resistance of the box base is [19]:

$$R_{cond} = \frac{t_{bottom}}{k_{box} A_{bottom}}$$

For the portion of base exposed to the coolant, thermal resistance is [19]:

$$R_{base} = \frac{1}{hA_{tubes}}$$

For a single fin, thermal resistance is: $R_f = (T_{fin\ base} - T_\infty)/q_f$

Total thermal resistance of all fins in parallel connection [19]:

$$R_{f,N} = \frac{T_{fin\ base} - T_\infty}{q_f} \frac{1}{N_f}$$

Where fin heat transfer rate for adiabatic tip is given by [19]:

$$q_f = \sqrt{hpk_{Al}A_c}\tanh(ml_f)\,(T_{fin\ base} - T_\infty)$$

Hence,

$$R_{f,N} = \frac{1}{\sqrt{hpk_{Al}A_c}\tanh(ml_f)} \frac{1}{N_f}$$

and

$$m = \sqrt{\frac{hp}{k_{box}A_c}}$$

$$A_c = t_f w_f$$

$$w_f = l_{tube}$$

$$p = 2(w_f + t_f)$$

Total thermal resistance from the battery base to the coolant:

$$R_{tot} = R_{contact} + R_{cond} + [\frac{1}{R_{base}} + \frac{1}{R_{f,N}}]^{-1}$$

Heat transfer rate:

$$Q_{cool} = \frac{T_b - T_\infty}{R_{tot}}$$

Where:

l_f: Fin length [m].

t_f: Fin thickness [m].

w_f: Fin width [m].

w_{tube}: Tube width [m].

l_{tube}: Tube length [m].

t_{bottom}: Box base thickness [m].

A_{bottom}: Total box bottom surface area [m^2].

A_{tubes}: Inner surface area of tubes upper surface [m^2].

$R_{contact}$: Thermal contact resistance between battery and box base [K/W].

R_{cond}: Thermal conduction resistance through box base [K/W].

R_{base}: Thermal convection resistance from tube inner top area [K/W].

$R_{f,N}$: Fins thermal resistance [K/W].

q_f: Heat transfer rate through fin [W].

p: Fin perimeter [m].

A_c: Fin cross-sectional area [m^2].

N_f: Number of fins.

T_∞: Coolant inlet temperature [K].

k_{box}: Box material conductive heat transfer coefficient [W/m.k].

h – Convective heat transfer coefficient [W/m^2 K].

Q_{cool}: Heat transfer rate from battery pack to the cooling fluid [W].

- **Calculating Convective heat transfer coefficient (h)** [19]**:**

$$h = \frac{Nu\ k_c}{D_h}$$

Where:

k_c: Thermal conductivity of the cooling fluid [W/m.K],

D_h: Tube hydraulic diameter and equals $(= \frac{4.Area}{Perimeter})$

Nu: Nusselt number.

To calculate the value of heat transfer convective coefficient h, it needs to calculate Nu value. There are different formulas that give Nu value for each case.

First Reynolds number is evaluated to know flow type:

$$Re = \frac{uD_h}{\nu}$$

Where:

Re: Reynolds number.

u: fluid inlet velocity [m/s].

ν: Kinematic viscosity of cooling fluid [m^2/s]

Nusselt number (Nu) depends on flow type, heat transfer condition and pipe shape, for inner flow, constant surface temperature; there are two case: for laminar flow Nu=3.66 and for turbulent flow smooth pipe Nu is given by [19]:

$$Nu = 0.023Re^{0.8}Pr^{0.4}\ (for\ 10^4 < Re < 10^6)$$

Where Pr is Prandtl number.

The above information can be used to find h value. Now everything is obtained to calculate heat transfer rate from the battery pack to the cooling fluid.

Energy balance equation of the system can be written as follows:

$$m_b C_{p,b} \frac{dT_b}{dt} = Q_b - Q_{cool} = I_b^2 R_i - \frac{T_b - T_\infty}{R_{tot}}$$

Rearranging, gives battery temperature change rate:

$$\frac{dT_b}{dt} = \frac{I_b^2 R_i}{C_b} - \frac{T_b - T_\infty}{C_b R_{tot}}$$

Where $\mathbf{C_b = m_b C_{p,b}}$ is battery thermal capacity [J/K].

The above equation can be used to calculate uniform battery temperature depending on the applied situation.

4. DESIGN OF EXPERIMENTS AND SIMULATION

In order to study the choices introduced earlier it is important to design a set of virtual experiments as well that best represent realistic situations that the vehicle might face. This includes:

- Driving cycle.
- Ambient temperature.
- Road slope

The first comparison to perform is the choice between LG and Samsung cells. Due to the crucial importance of overheating problem, this test will be based on thermal dissipation of each cell to see which cell will reach higher temperatures in these situations. In this simulation, no cooling is assumed. After choosing the best battery cell, the overall performance of the designed battery pack with the cooling system either using ambient air or cooled air will be studied.

Driving cycle:

It is important to define the velocity ranges and variations that the vehicle should perform. Since the vehicle is intended to be used mainly as an urban electric car, lower velocity ranges are more of interest. For this reason, the Low-Medium (first 1000 seconds) part of WLTP Class 3 is chosen to be put into the simulations as the reference driving cycle and it is repeated for 3200 seconds. The choice of 3200 seconds is because in extreme conditions the SOC of the battery reaches very low values. Therefore, it was chosen for all the set of conditions to have comparable results.

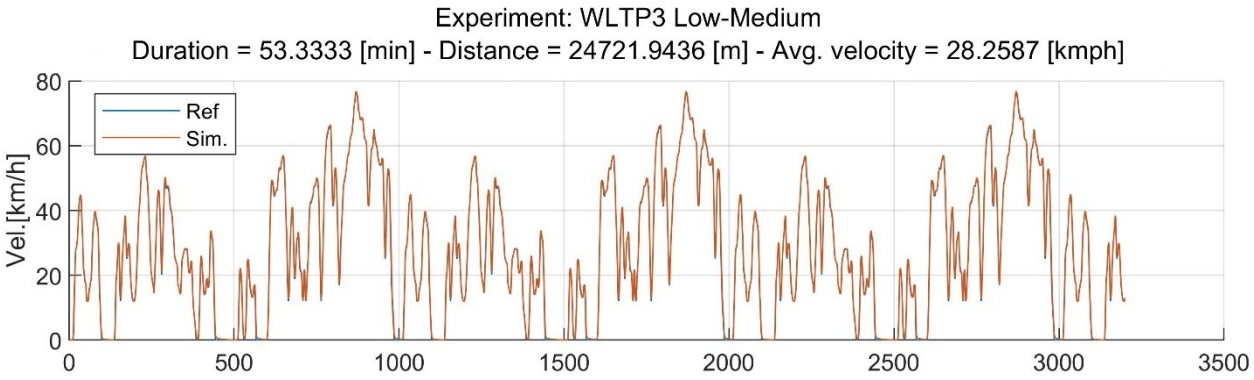

Figure 4.1: Driving cycle.

Ambient temperature:

Variations of atmospheric temperature during the year and between different regions affect the rate of heat rejection from battery to atmosphere, which affect the ability of battery cooling especially when it comes to ambient air cooling. Hence, the maximum temperature battery can reach during a driving cycle. So it is important to evaluate the efficiency of each cooling system in all conditions.

A set of ambient temperatures are chosen to be studied:

- 5 ºC
- 15 ºC
- 25 ºC
- 35 ºC
- 40 ºC

At values lower than 5 ºC the battery needs to be heated by a dedicated heater before driving.

Road slope:

Depending on road grade, higher torque could be required from the motor. Consequently, higher current from the battery. This increases dissipation in both motor and battery that in turns increases their temperatures. A set of road slopes are considered:

- -10 %
- -5 %
- 0 %
- 5 %
- 10 %

Values over 10 % are over estimation form road construction point of view.

Battery thermal parameters:

LG: $C_b = 3.0078*10^4$ J/K

Samsung: $C_b = 4.0772*10^4$ J/K

From the aforementioned cases, all possible combinations of ambient temperatures and road slopes are simulated and studied. No deration will be used in these simulations.

4.1 Thermal dissipation of battery cells

A comparison is carried out between thermal dissipation of the two proposed battery cells. In this study, no cooling is assumed thus the total generated thermal energy heats up the battery and results in temperature increase. Hence, it gives an idea about thermal characteristics of each cell without other effects.

- Average dissipated thermal energy:

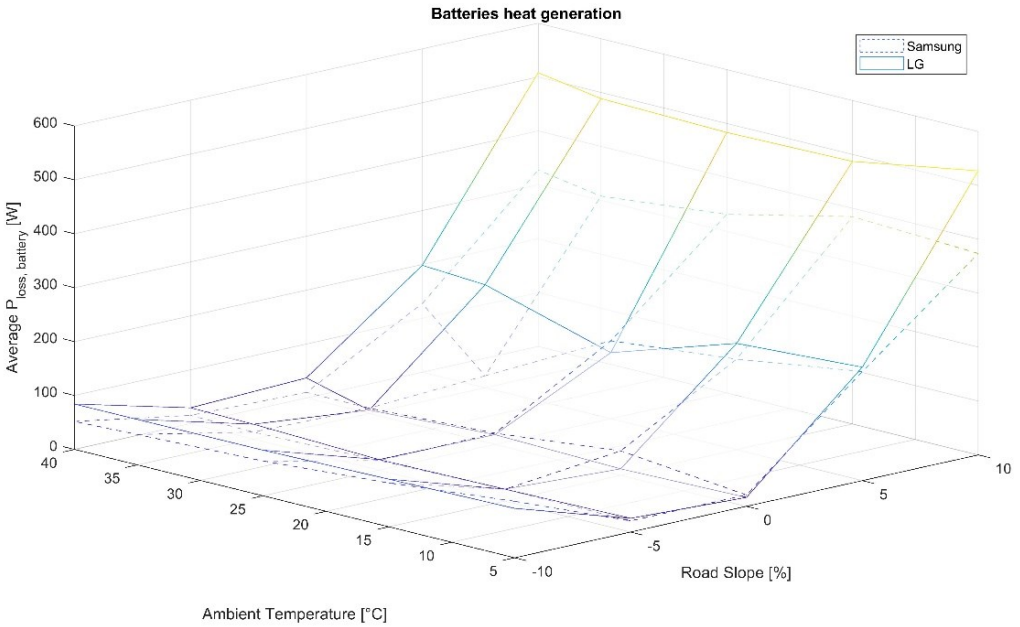

Figure 4.2: Average heat generation of LG and Samsung battery cells.

- Maximum battery temperature:

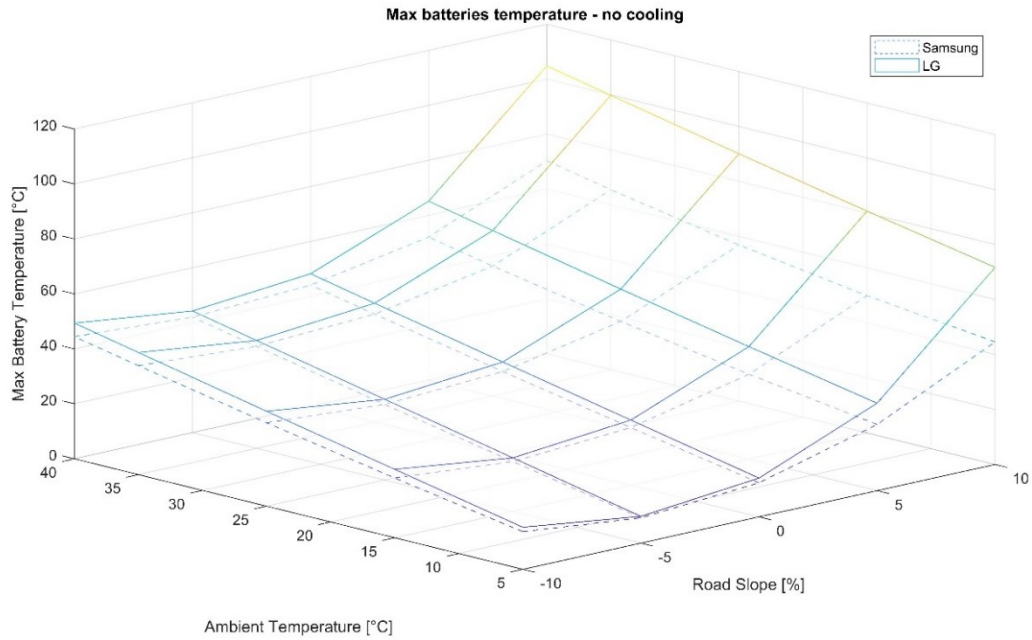

Figure 4.3: Maximum temperature of LG and Samsung battery cells.

It is obvious that LG cell produces more heat. Moreover, the difference increases with road slope. Since LG produces more heat, it reaches higher temperatures, which increase with road slope and ambient temperature increase. In addition, LG reaches dangerously high temperatures at extreme conditions. Whereas Samsung maintains lower temperatures. On the other hand each cell has its own threshold temperature limit and should be compared to that limit.

It is useful to know as well how much time of the driving cycle each battery cell exceeds the maximum safe temperature limit.

- Battery overheat duration:

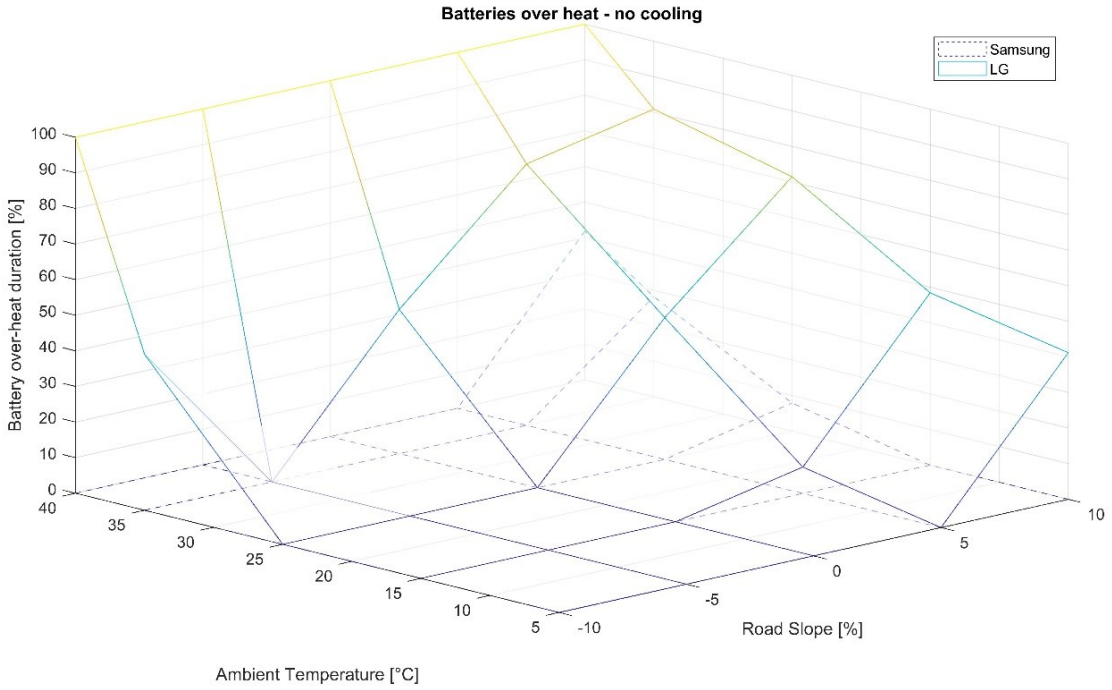

Figure 4.4: Battery overheat duration.

LG becomes overheated for almost half of the situations and it lasts for the whole cycle in the cases where ambient temperature is high. Whereas Samsung passes temperature threshold only in cases of uphill road slope greater than 5% and it lasts much less than equivalent LG cases. This shows the superior performance of Samsung cells over LG cells.

Final decision: Samsung Prismatic cells.

From now on, any further analysis will be carried out assuming Samsung prismatic cells are used. After making the choice, it is time to study the effect of cooling system. Finally, the de-rate strategy in extreme situation will be studied.

4.2 Cooling system

After the previous experiments of no cooling case, Samsung cell is chosen for the battery pack. However, in reality a cooling effect is present either forced convection by ambient air forced by car speed or by cooled air from an air conditioning system. In this section, the behavior of Samsung prismatic cells will be studied in maximum performance conditions without any deration and results are represented.

4.2.1 Ambient air cooling:

In this system, forced convection cooling is performed by ambient air forced by car speed through the tubes in the bottom of the battery pack box combined with a dedicated fan at a speed lower than 10 km/h. Simulation is performed assuming the previously mentioned conditions of road slope and ambient temperature.

- **Evaluation of air properties**[19]**:**

Air properties are taken at an average temperature 27 ºC:

Density: $\rho = 1.1614\ kg/m^3$

Kinematic viscosity: $\nu = 1.589 * 10^{-5}\ m^2/s$

Specific heat: $C_p = 1007\ J/kg.K$

Thermal conductivity: $k = 0.0263\ W/m.K$

Prandtl number: $Pr = 0.707$

- Average cooling power achieved and average battery heat generation:

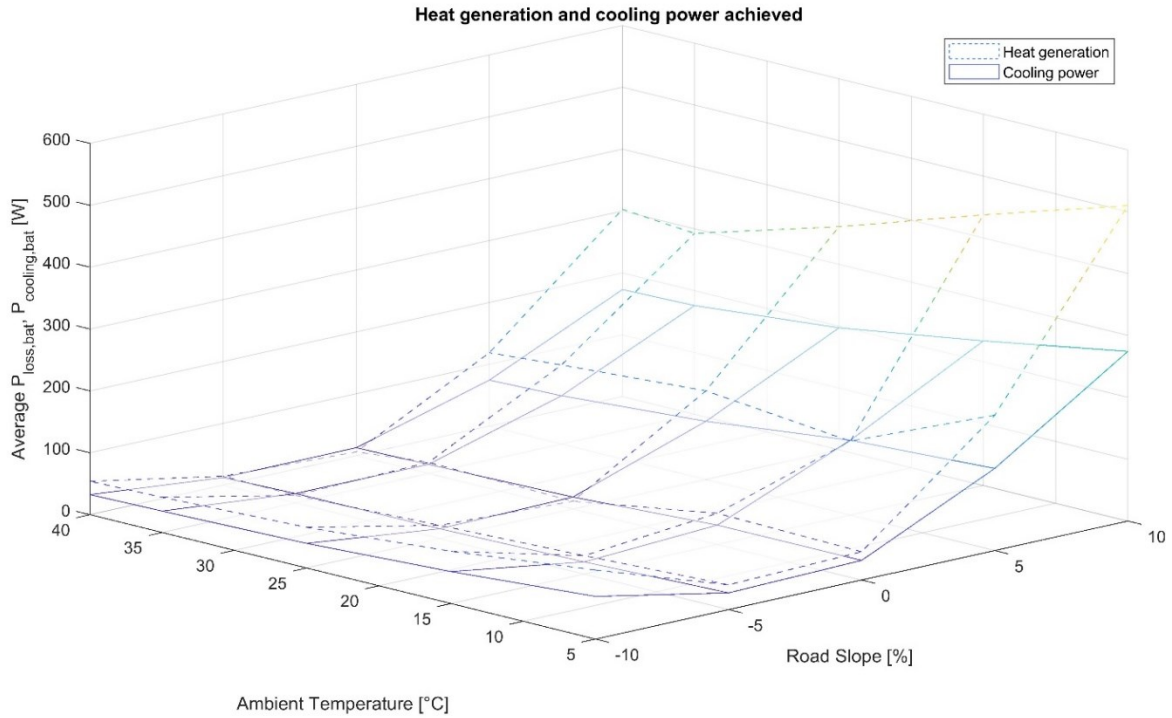

Figure 4.5: Average cooling power and average battery heat generation – ambient air.

The difference between cooling power and heat generation is small in normal conditions but it becomes larger in extreme conditions e.g. high road slope.

- Maximum battery temperatures:

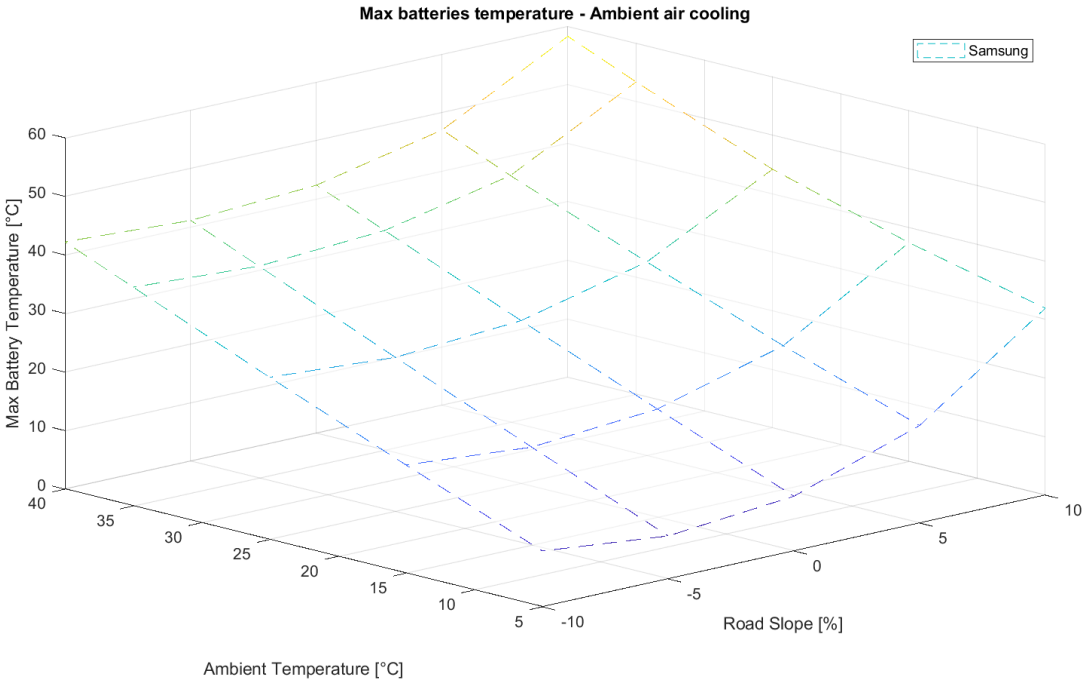

Figure 4.6: Maximum battery temperatures – ambient air.

- Battery overheat duration:

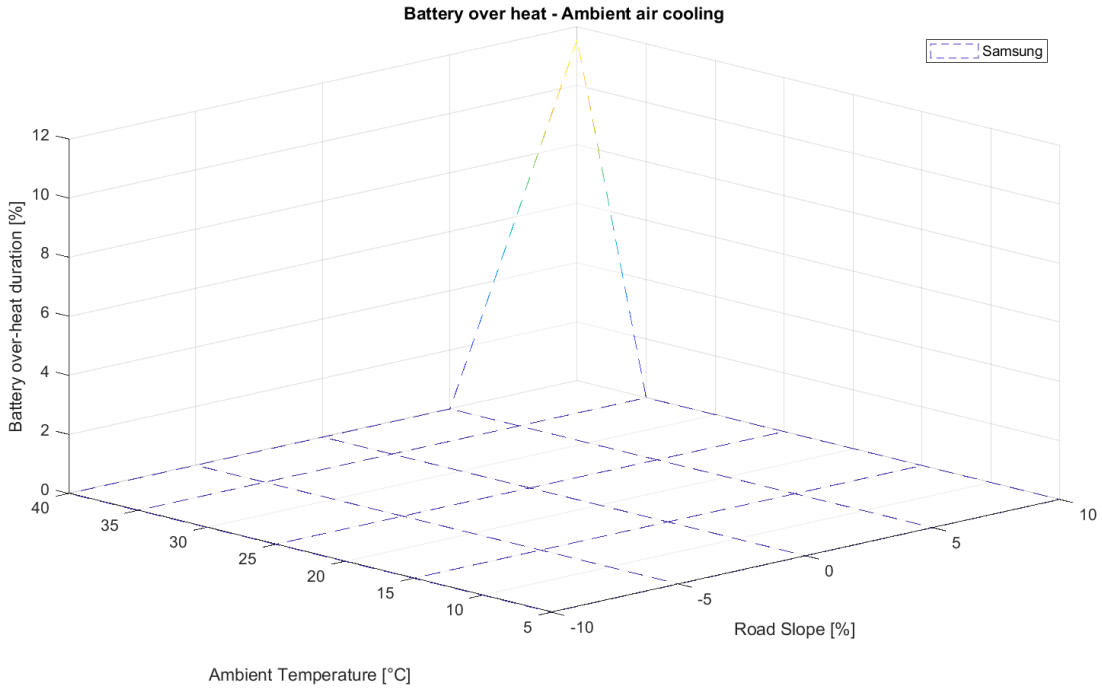

Figure 4.7: Battery overheat duration for every condition – ambient air.

As evident from figure 4.7, Samsung is always below the danger temperature limit except for an extreme case of ambient temperature 40 ºC and road slope 10%.

4.2.2 Cooled air:

It is a closed cooling system with air cooled to an assumed temperature **15ºC** by a dedicated air conditioner and flowing by a fan with a constant speed **3 m/s**.

- Average cooling power achieved and average battery heat generation:

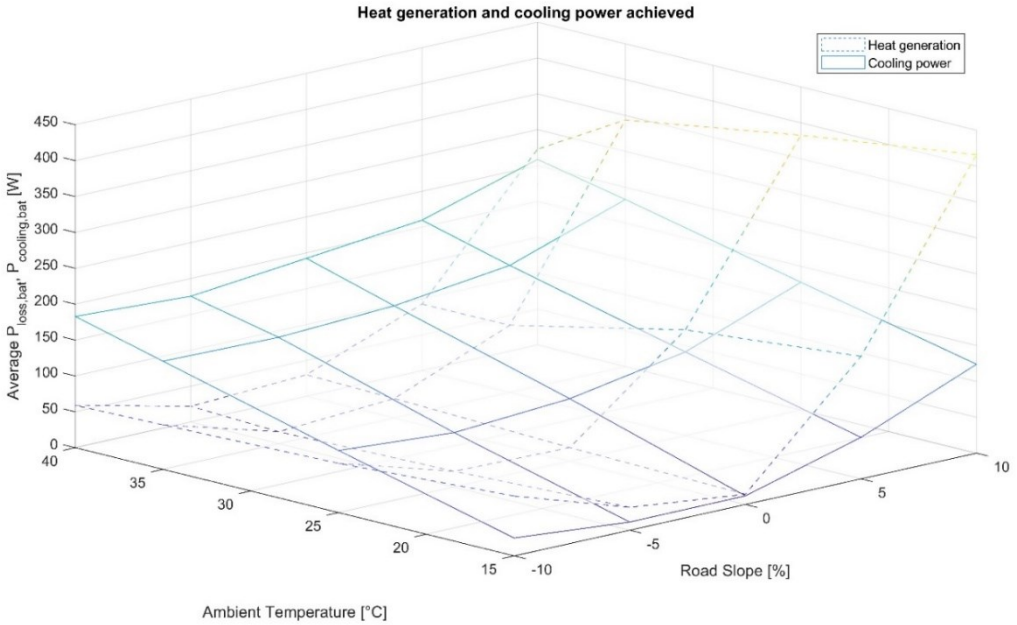

Figure 4.8: Average cooling power and average battery heat generation – Cooled air.

- Maximum and average battery temperatures

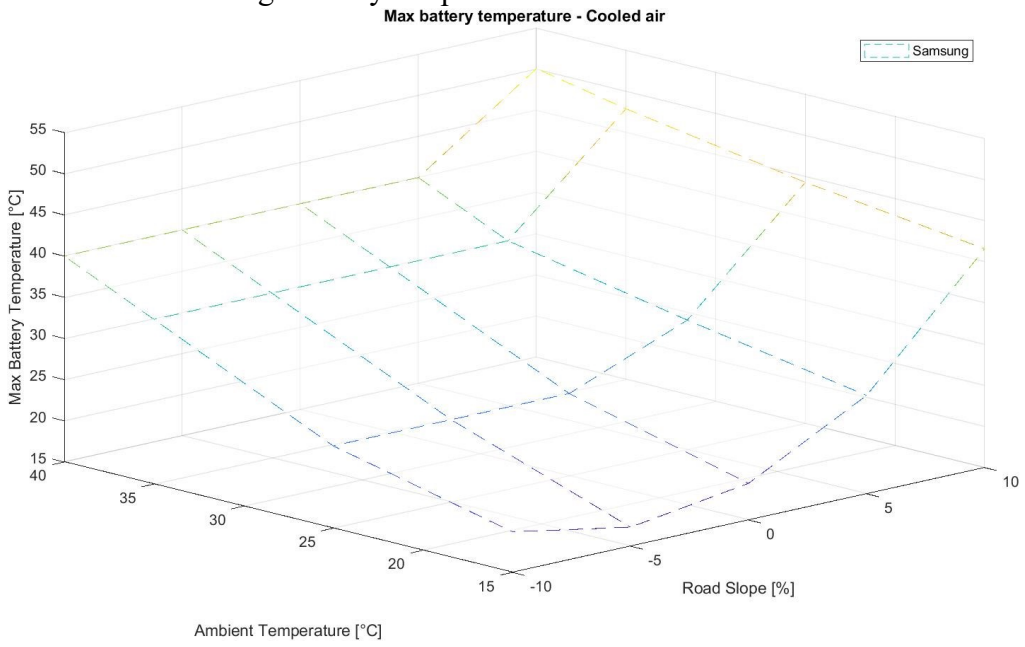

Figure 4.9: Maximum and average battery temperatures – Cooled air.

It is obvious that in this case battery does not overheat at all and it only reached 50 ºC in a one extreme case of road slope 10% and ambient temperature 40 ºC.

5. PREDICTION AND DERATION

So far in the design phase the analysis and the choices regarding battery cell type and cooling system have been made. As the next step, the goal is to deal with the overheating problem in a more sophisticated way rather than simply relying on the battery's thermal characteristics or cooling capabilities.

BMS settings by default contain passive safety measures when the battery is overheated. In this situation, the current passing through battery will be limited by the BMS becoming eventually zero in extremely overheated conditions, which means the vehicle becomes completely useless. The proposed solution in this thesis is to tackle this issue by acting in anticipant way through predicting the battery temperature in the near future e.g. next 5 minutes and making proper changes in the inverter settings in advance such that the anticipated overheating could be avoided.

Prediction

Assuming that the near future is also characterized almost by the same driving style that was being used in the specified past window, it will be possible to make predictions of the upcoming situations. The prediction system stores the dissipation values of the battery pack and the electric motor. Next, by finding the moving average of these dissipations in the specified past time window, the future temperatures are calculated according to the thermal modellings of the battery pack and the motor. It is assumed that in the prediction horizon motor and battery will continuously give the mean of these values. Then this procedure is repeated continuously according to the specified updating interval.

A MATLAB Simulink function is used for this procedure, figure 5.1. The function pauses the simulation at the end of every update interval to perform the computation. Whereas during simulation running the aforementioned values are stored.

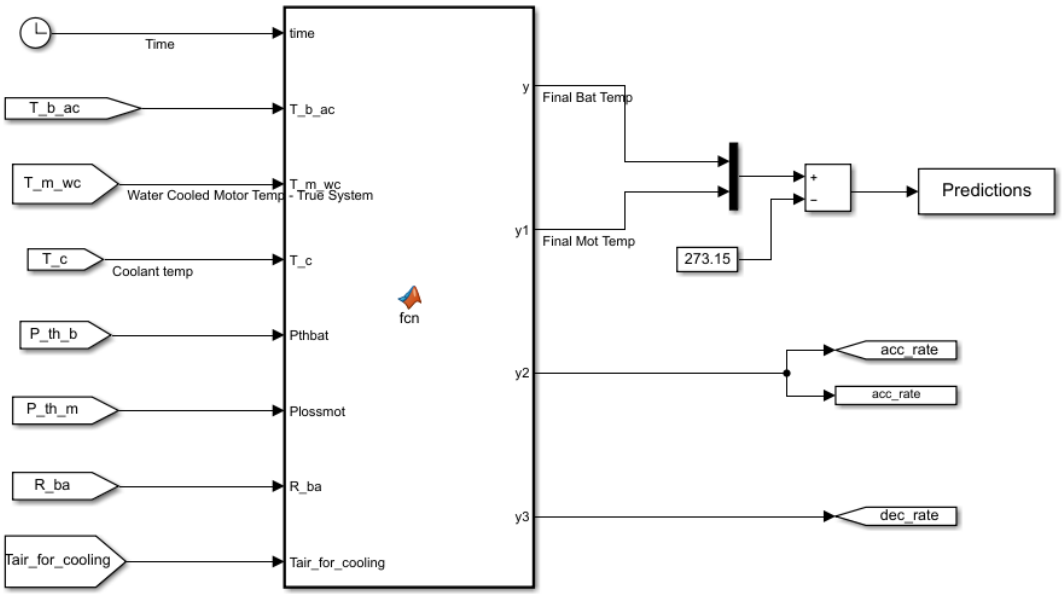

Figure 5.1: MATLAB Simulink prediction function.

5.1 Motor prediction

To know how motor temperature changes it is necessary to understand how much is the thermal dissipation, which depends on the motor torque while the rest parameters are either constants or are obtainable through iteration.

At each prediction instance:

- Q_m mean value is calculated for the history time length and is considered fixed for the whole prediction horizon.
- Actual motor, coolant and ambient temperatures are read.
- Through mathematical iteration the final predicted temperature at the end of the horizon is obtained.

$$\frac{dT_m(t)}{dt} = \frac{Q_m(t)}{C_m} - \frac{Q_{cool,m}(t)}{C_m} = \frac{Q_m(t)}{C_m} - \frac{T_m(t) - T_c(t)}{C_m R_{mc}}$$

$$\frac{dT_c(t)}{dt} = \frac{T_m(t) - T_c(t)}{C_c R_{mc}} - \frac{Q_r(t)}{C_c} = \frac{T_m(t) - T_c(t)}{C_c R_{mc}} - \frac{k_r A_r}{C_c}(T_c(t) - T_{amb})$$

Where:

Q_m – Motor heat generation rate [W] -> system input

T_m – Motor temperature [K] -> state variable/system output

T_c – Motor coolant temperature [K] -> state variable

T_{amb} – ambient temperature [K] -> system input (measured disturbance)

R_{mc} – Thermal resistance between motor and coolant [K/W]

C_m – Motor thermal capacity [J/K]

C_c – Motor coolant thermal capacity [J/K]

k_r – Radiator thermal transfer coefficient [W/m^{2}K]

A_r – Radiator frontal area [m^2]

System constants

5.2 Battery prediction

Also, battery temperature depends on its dissipation which depends on the current drawn from the battery. In order to perform the prediction similar to what was done for motor; the mean value of dissipation history is considered as the constant dissipation value that battery will continuously give for the whole prediction horizon.

$$\frac{dT_b(t)}{dt} = \frac{Q_b(t)}{C_b} - \frac{Q_{cool,b}(t)}{C_b} = \frac{Q_b(t)}{C_b} - \frac{T_b(t) - T_{amb}}{C_b R_{ba}}$$

Where:

Q_b – Battery heat generation rate [W] -> system input

T_b – Uniform battery temperature [K] -> state variable/system output

T_{amb} – ambient temperature [K] -> system input (measured disturbance)

R_{ba} – Thermal resistance between battery and air [K/W]

C_b – Battery thermal capacity [J/K]

} System constants

Example of prediction:

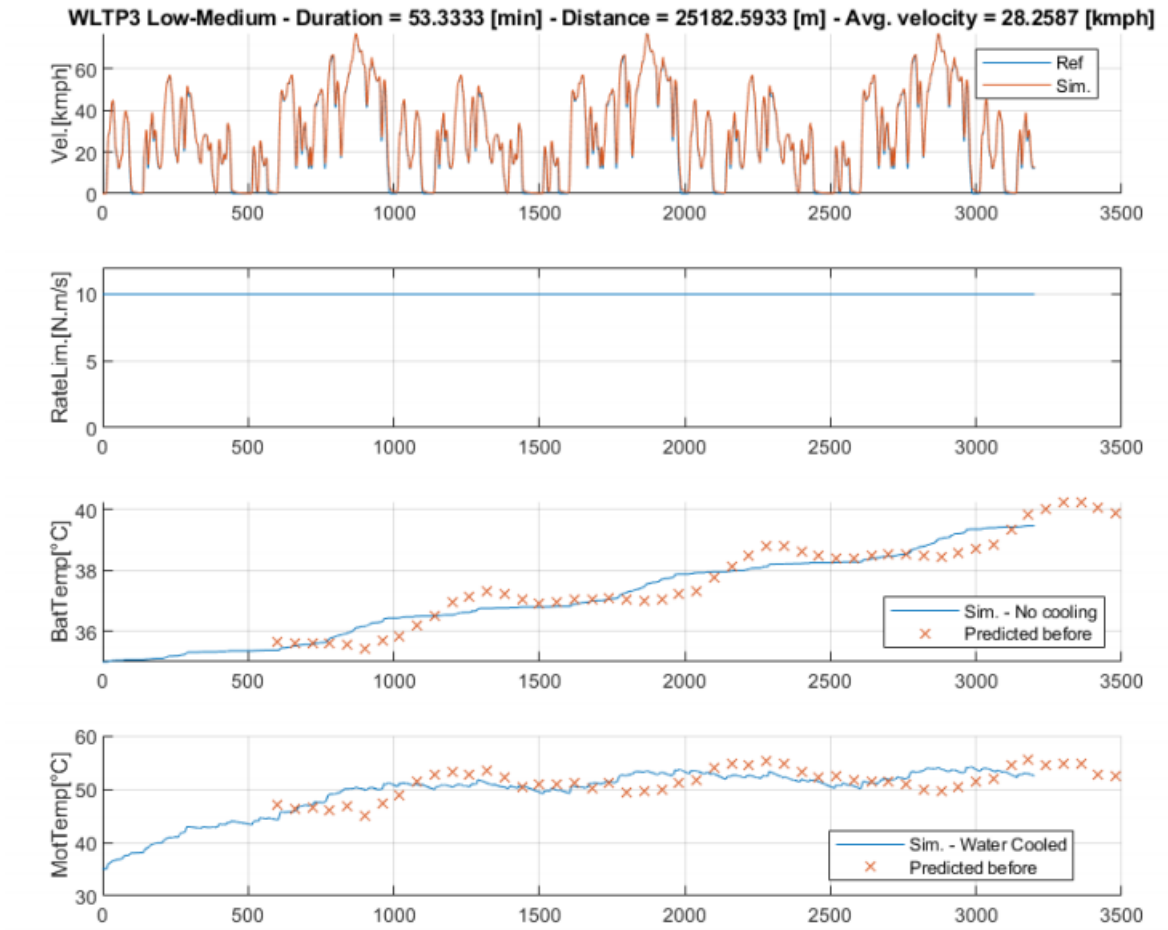

Battery Pack = Samsung
Ambient temp [°C] = 35
Slope [%] = 0
Prediction horizon [s] = 300
History window [s] = 300
Update interval [s] = 60
Limit bat temp [°C] = 55
Battery Cooling = No cooling
Constant Sportive: 10 [N.m/s]

Vel. error rms [kmph] = 2.1699
Bat. temp. error rms [°C] = 0.40712
Mot. temp. error rms [°C] = 2.2804
Max bat. temp [°C] = 39.471
Max mot. temp [°C] = 54.1821
Spec. cons. w/ & w/o reg. [Wh/km] =93.6199 - 113.884
Final SOC [%] = 78.9322
Bat. overheat duration [%] = 0

Figure 5.2: Example of prediction.

5.3 Prediction accuracy

Before the implementation of prediction strategy, it is important to study the reliability of the values coming from prediction by evaluating the error between the real values and the values predicted before. Factor could affect prediction accuracy are:

- Time history length.
- Prediction horizon length.
- Used statistical quantities:
    - Mean
    - RMS

5.3.1 Prediction horizon length

Length of prediction horizon depends heavily on the dynamics of the system. Thermal dynamics of both battery and motor have been simplified in the form of LTI systems so it is possible to observe the step response of the systems as the following:

Battery

$$\{\dot{T}_b(t)\} = \left[-\frac{1}{C_b R_{ba}}\right]\{T_b(t)\} + \left[\frac{1}{C_b} \quad \frac{1}{C_b R_{ba}}\right]\begin{Bmatrix} Q_b(t) \\ T_{amb} \end{Bmatrix}$$

Parameters in battery prediction equation are obtained from the actual vehicle and ambient air cooling system. Step response shows that the system has an extremely large time constant (around 30000 seconds)

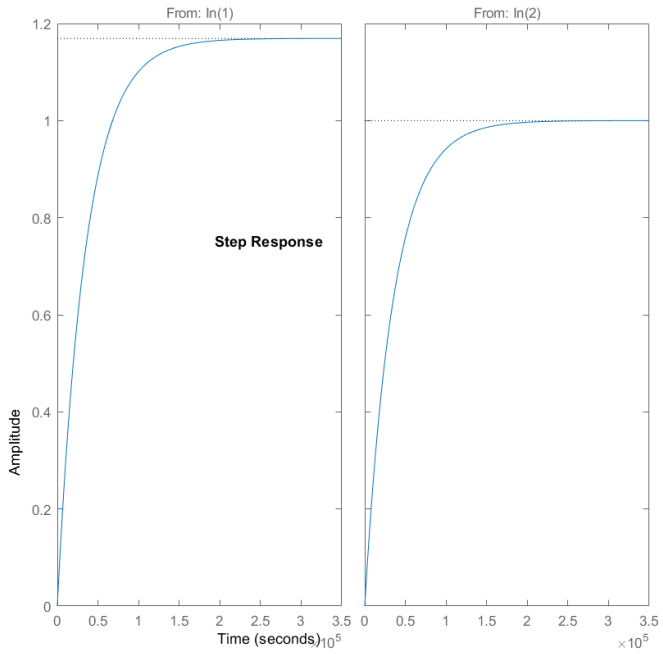

Figure 5.3: Step response of battery thermal dynamics.

Motor

$$\begin{Bmatrix} \dot{T}_m(t) \\ \dot{T}_c(t) \end{Bmatrix} = \begin{bmatrix} -\frac{1}{C_m R_{mc}} & \frac{1}{C_m R_{mc}} \\ \frac{1}{C_c R_{mc}} & -\frac{1}{C_c R_{mc}} - \frac{k_r A_r}{C_c} \end{bmatrix} \begin{Bmatrix} T_m(t) \\ T_c(t) \end{Bmatrix} + \begin{bmatrix} \frac{1}{C_m} & 0 \\ 0 & \frac{1}{k_r A_r} \end{bmatrix} \begin{Bmatrix} Q_m(t) \\ T_{amb} \end{Bmatrix}$$

In case of motor it reaches stability much faster than the battery. It can be seen from step response of the motor thermal dynamics, time constant of the system is about 4800 seconds. This is also justifiable by looking at the eigenvalues of the dynamic matrix (-0.0017, -0.0039).

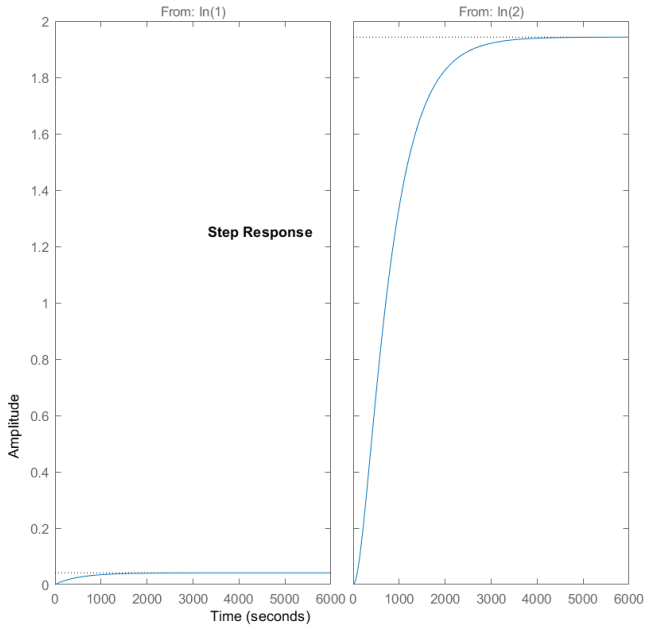

Figure 5.4: Step response of motor thermal dynamics.

Comparison between different prediction horizon values

Considering system time constants discussed before, three values of prediction horizon are compared together: 3 minutes, 5 minutes, and 10 minutes. Other factors are fixed. For every simulation time history window of 300 seconds, road slope 10% and ambient temperature 25°C. Results and temperature prediction errors are represented.

1st: Prediction horizon 3 minutes (180 seconds)

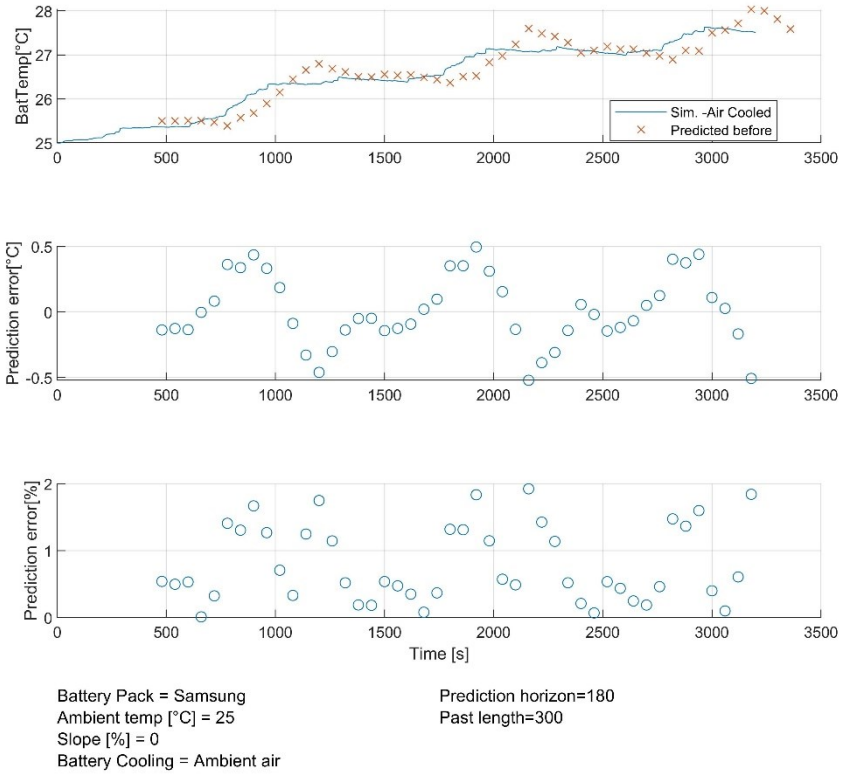

Figure 5.5: Temperature prediction error of 180 seconds prediction horizon.

2nd: Prediction horizon 5 minutes (300 seconds)

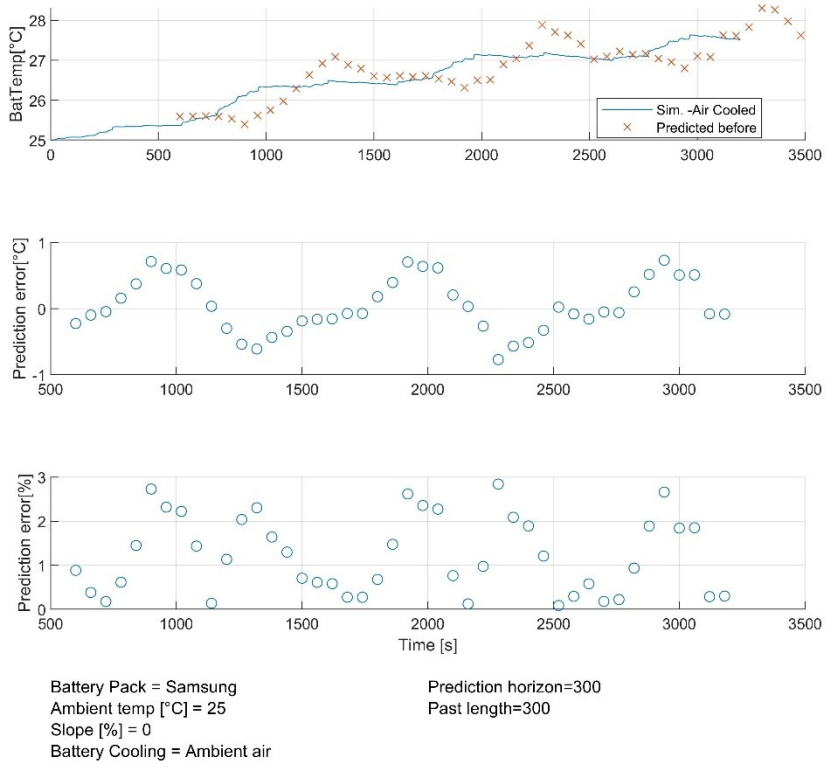

Figure 5.6: Temperature prediction error for 300 seconds prediction horizon.

3rd: Prediction horizon 10 minutes (600 seconds)

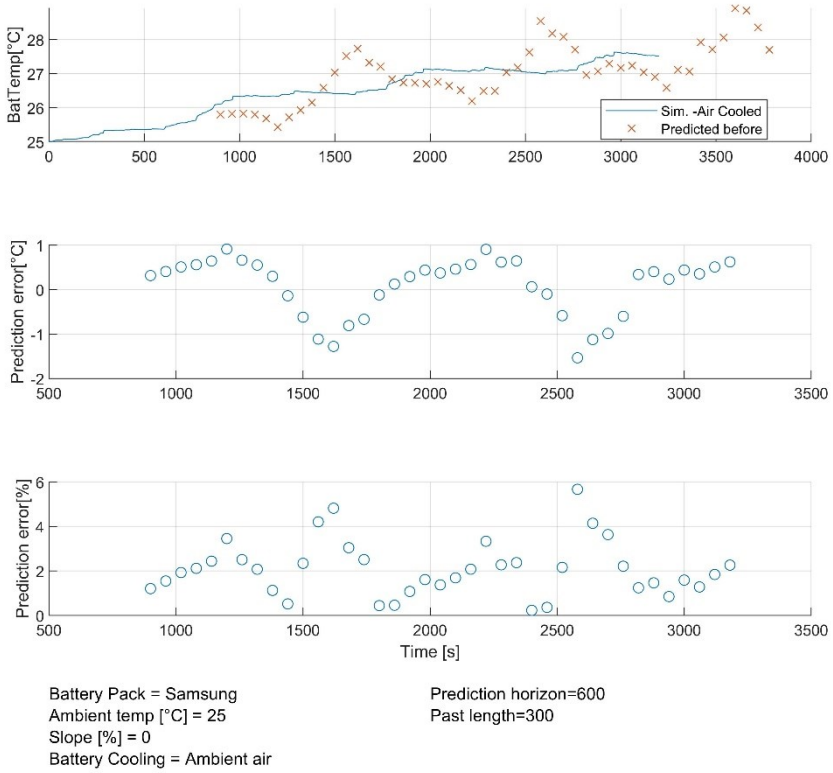

Figure 5.7: Temperature prediction error for 600 seconds prediction horizon.

As observed from the graphs prediction error is relatively small and error percentages are close to each other for 3 minutes and 5 minutes prediction horizon whereas it becomes larger for 10 minutes prediction horizon. In addition, error percentage becomes larger with increasing road slope. Therefore, the best value to choose is 5 minutes (300 seconds) prediction horizon. This value will be used for the introduced prediction/deration strategy.

5.3.2 Time history length

Same as prediction horizon length, the length of time history window along which the average values of driving behavior are evaluated affects the magnitude of temperature prediction error. By fixing the other factor and prediction horizon on 5 minutes (300 seconds) different values of the time history window will be compared: 3 minutes (180 seconds) and 5 minutes (300 seconds). It is important to note that, the length of time history window depends also on another factor which is the driving cycle. So, this value is cycle dependent variation of the driving cycle can affect the best value, shorter or longer one can be needed for different driving conditions.

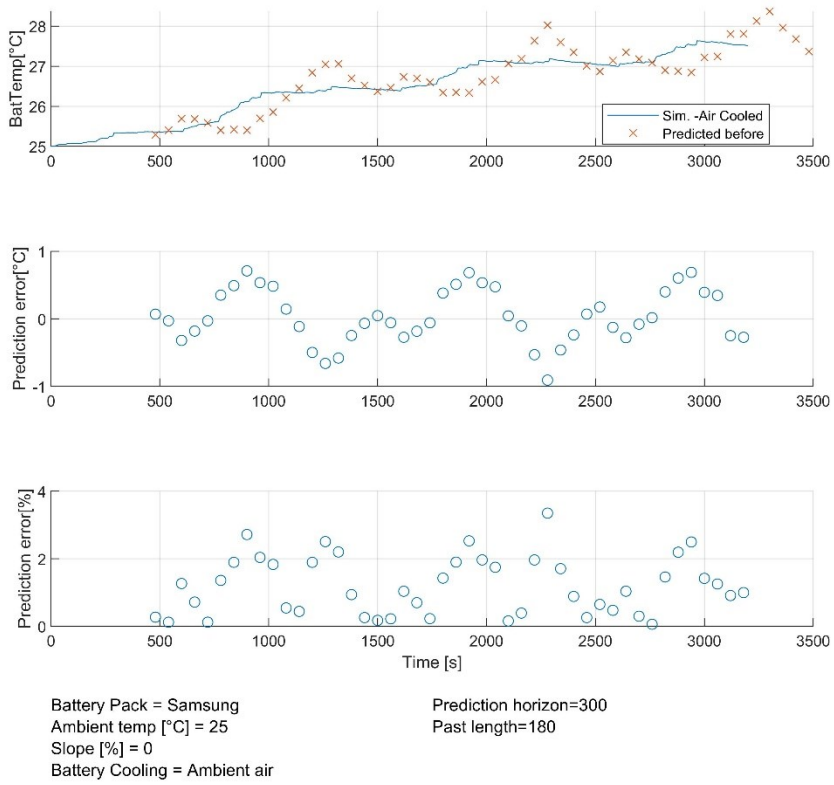

Figure 5.8: Temperature prediction error for 180 seconds time history length.

Result of time history 300 seconds is introduced before. The chosen value is 5 minute (300 seconds) time history as prediction accuracy is slightly higher.

5.4 Deration

So far the battery pack was selected and ambient air cooling is tested and showed an improvement in terms of battery overheating yet overheating still occurs at an ambient temperature 40 ^{o}C and road slope 10%. So a different de-rate strategy will be exploited in order to solve this overheating problem. After predicting battery and motor temperatures, this information is used to limit temperature increase by deration.

Battery current is related to motor torque as follows:

$$I_b = \frac{Mech.power + Losses}{Battery\ voltage} = \frac{\tau_m \omega_m + Q_m}{V_T}$$

Mainly motor torque defines how much current is required from the battery, so it is reasonable to focus on de-rating motor torque to avoid battery overheating.

5.4.1 Studied de-rate strategies:

- **Limiting maximum available motor torque:**

In this strategy, motor torque is limit according to thermal characteristics of the battery. Thus, battery overheating will be avoided for granted mathematically. The main problem with this strategy was the fact that maximum motor torque at high temperature situations has to be limited to very low values. In this way, the driver will get extremely limited and the situation will not be so much different from the passive safety feature of the BMS itself where vehicle becomes useless.

- **Limiting maximum rate of change in motor torque:**

By limiting the rate of change of the torque, the maximum available motor torque values are the same but what differs is the rate of the variations in motor torque i.e. how fast motor torque increases from the current value to the one requested by the driver. It is like a filter between drivers command and the value transmitted to the motor. The disadvantage of this strategy is the fact that it is not directly connected to the battery temperature through mathematical equations which brings along some uncertainty. This is the chosen strategy and its performance will be studied in the results below.

In order to specify maximum rate limits, three driving modes are introduced:

- **Sportive:** maximum rate of change 10 N.m/s.
- **Standard:** maximum rate of change 5 N.m/s.
- **Economy:** maximum rate of change 1 N.m/s.

Example of deration:

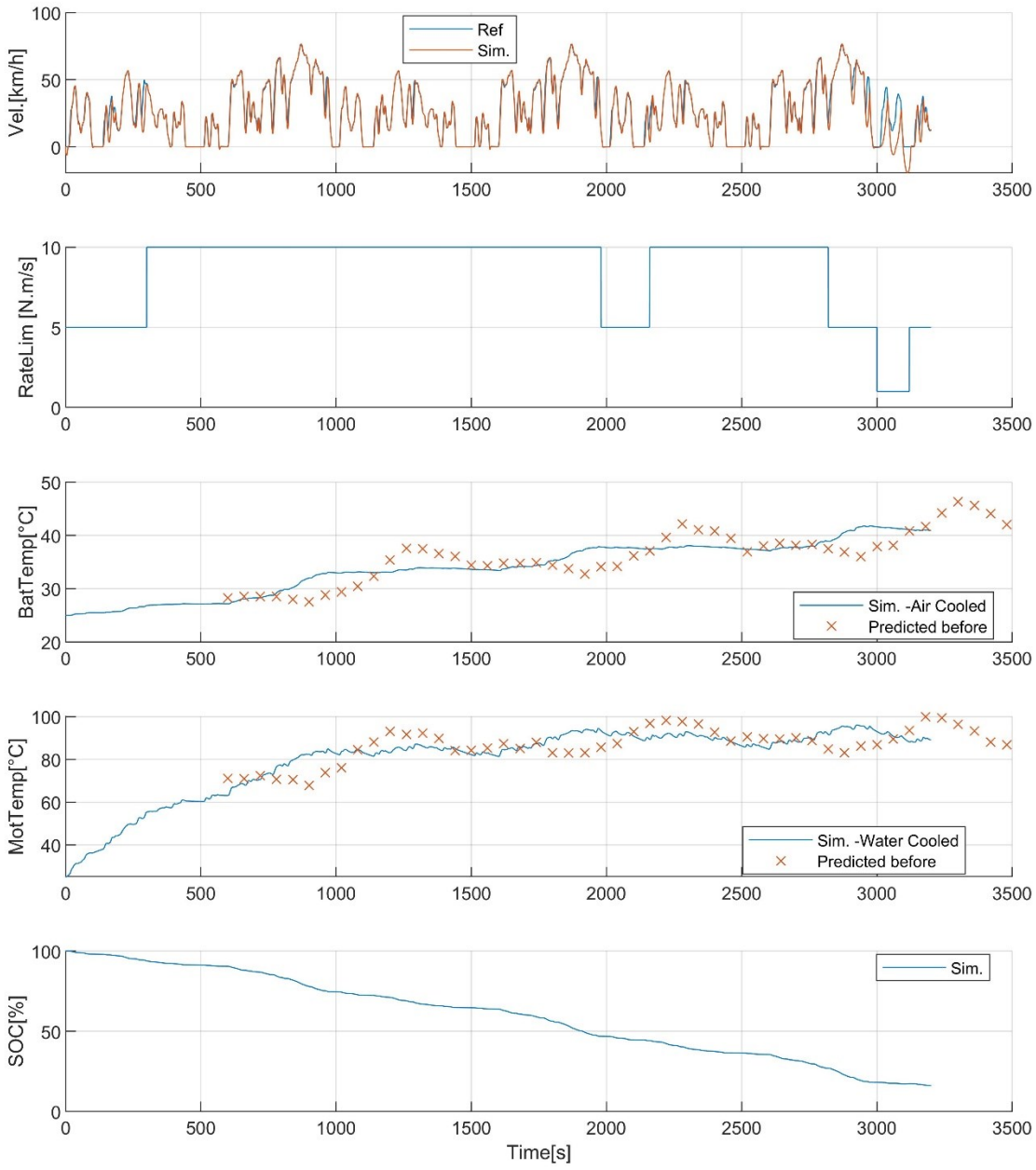

Figure 5.9: Example of deration – road slope 10%, ambient temperature 25 ºC.

Variation of motor torque increase rate is shown. As stated, when prediction algorithm predicts a high battery temperature in the future, it gives a command in the present to set motor torque increase rate to lower value, this is more evident in the two instances when the predicted battery temperature is bigger than 40 ^{0}C.

5.4.2 Implementation:

Battery temperature is predicted for the next 5 minutes according to its performance in the previous time length and the predicted values are updated every 60 seconds. Based on the difference between predicted temperature and the overheating threshold of the battery a driving mode is chosen as follows:

- More than 15 ºC difference: **Sportive** mode.
- Between 10 to 15ºC difference: **Standard** mode.
- Less than 10 ºC difference: **Economy** mode.

Figures 5.10, 5.11 show rate limiter in case of deration activated:

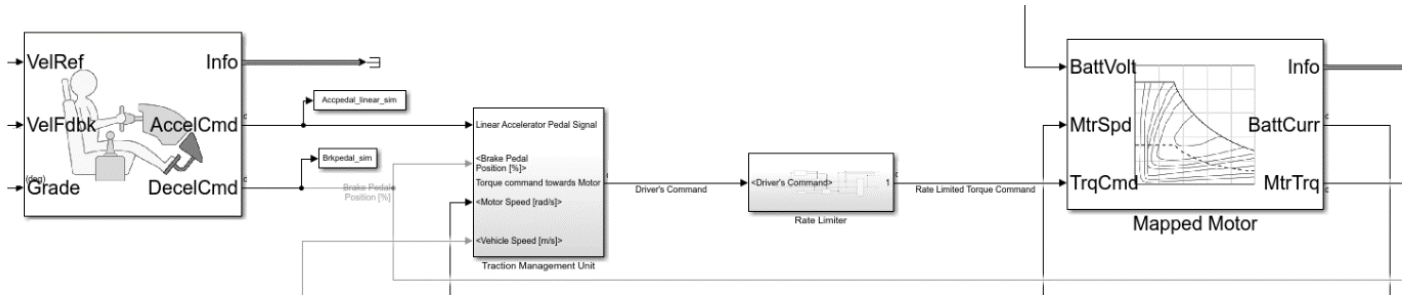

Figure 5.10: Torque rate limiter between driver's command and motor.

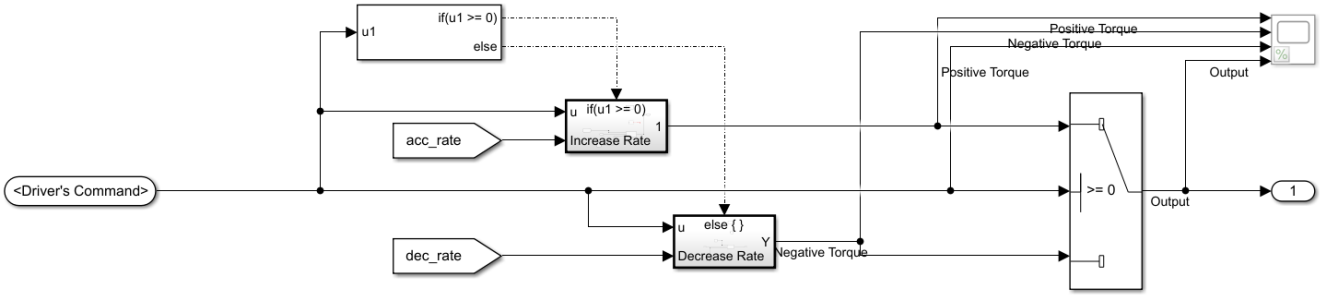

Figure 5.11: Torque rate limiter.

5.4.3 No cooling:

It is a good measure of the derate strategy effectiveness to test it with the no cooling case to observe the amount of improvement in the results especially in terms of maximum battery temperature and battery overheating duration.

The following simulations will be performed assuming no cooling as before but with deration to compare results.

- Average battery heat generation:

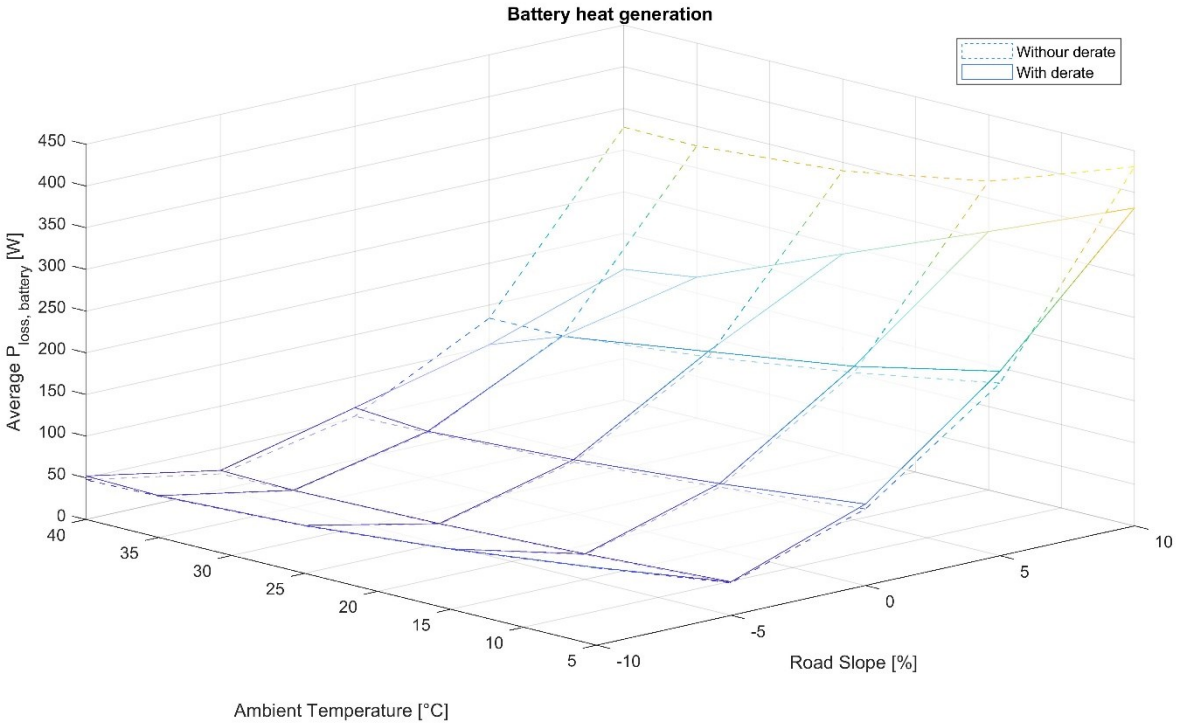

Figure 5.12: Average battery heat generation – no cooling.

There is a big reduction in heat generation inside the battery due to its internal losses. This will reflect on battery maximum temperature as well.

- Maximum battery temperatures:

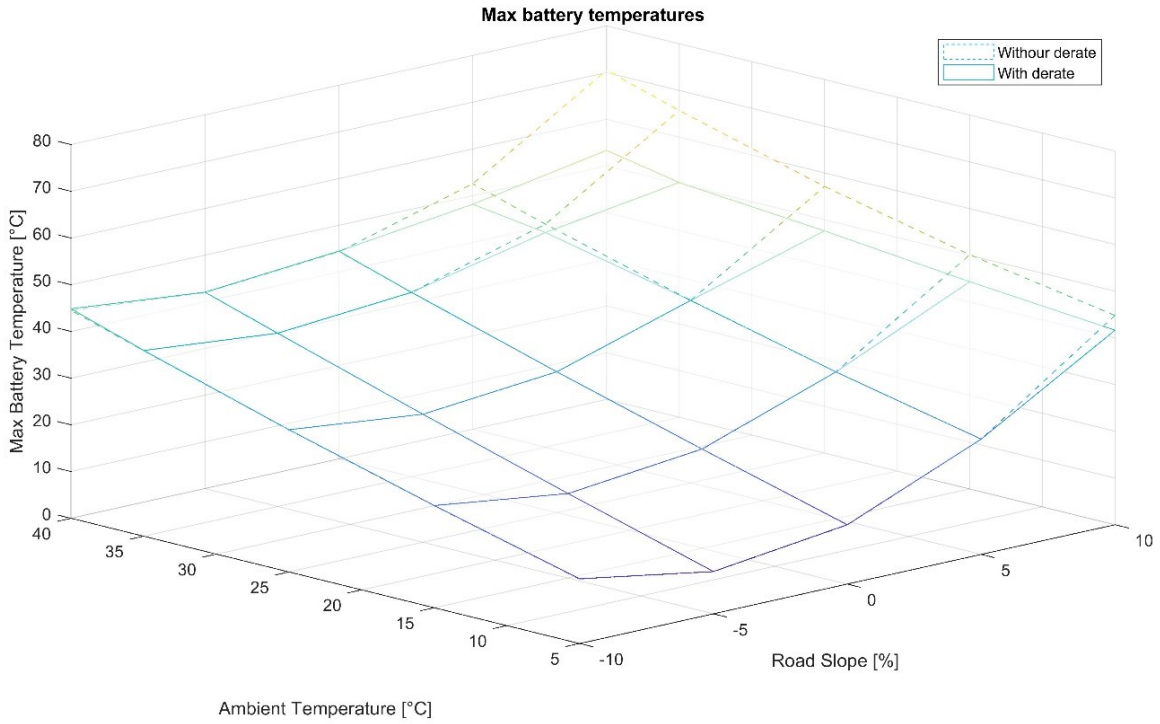

Figure 5.13: Maximum battery temperatures – no cooling.

Here it can be seen that the battery temperature with deration is always below the threshold, which solves the overheating problem even with no cooling.

- Battery overheating duration:

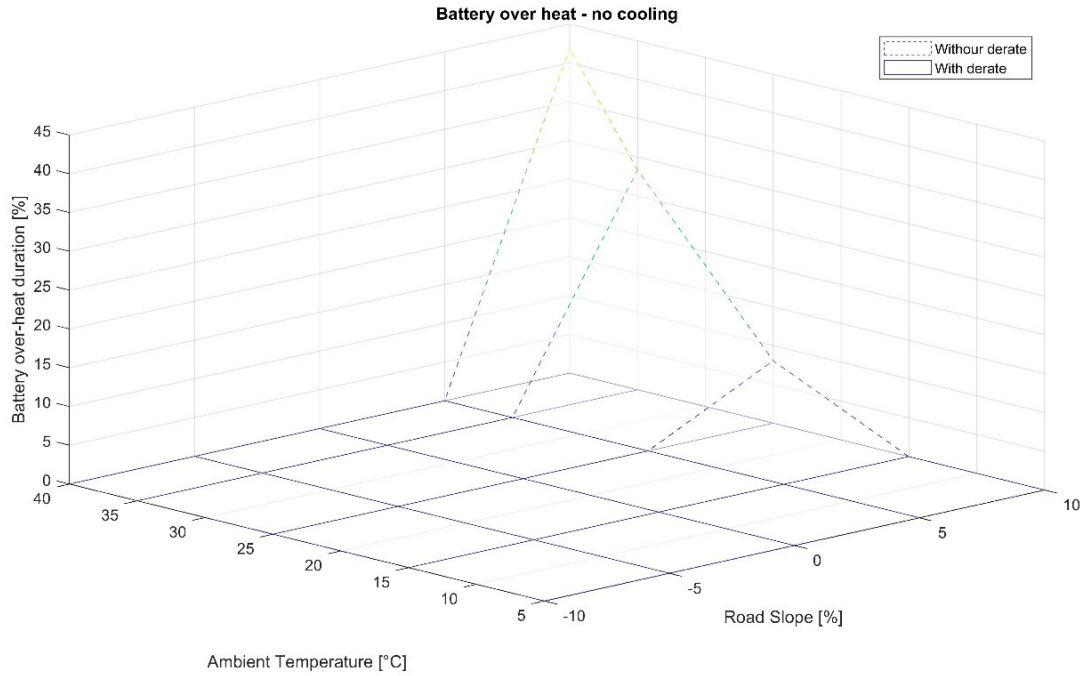

Figure 5.14: Battery overheating duration – no cooling.

- Consumption:

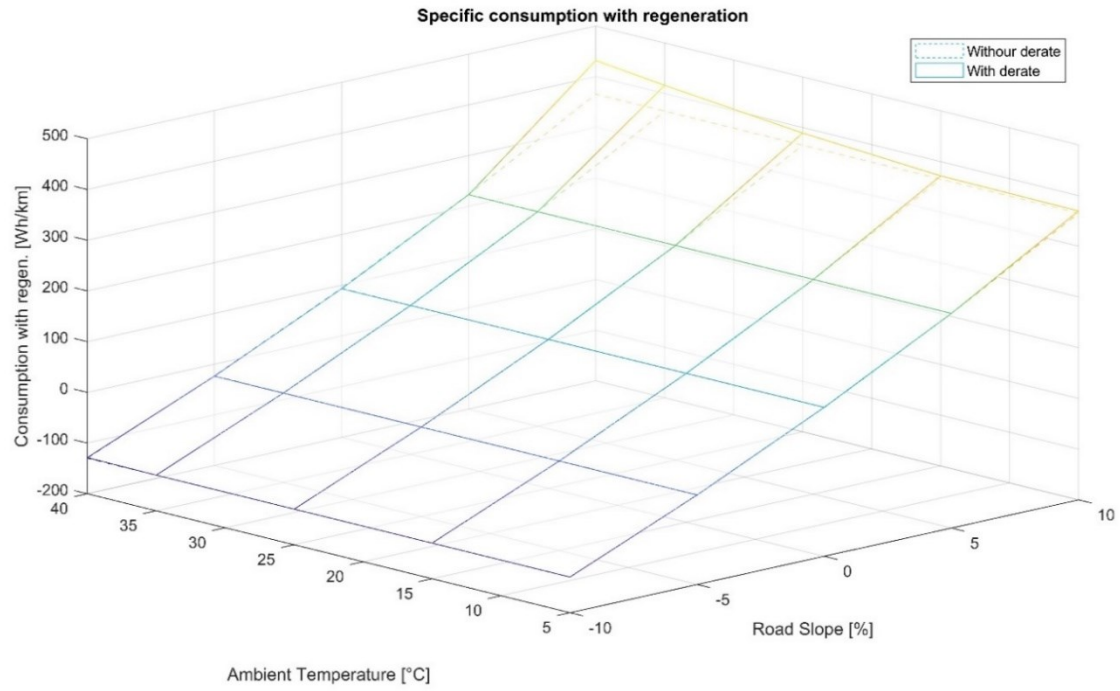

Figure 5.15: Specific consumption with regeneration – no cooling.

- Battery final SOC:

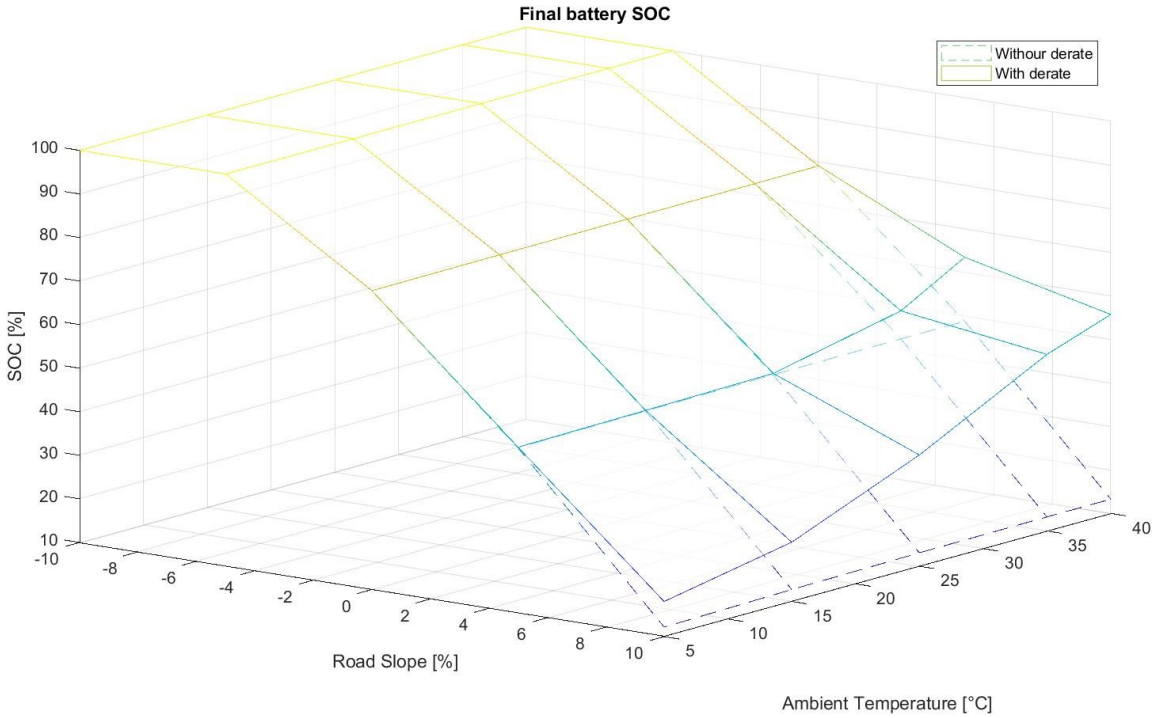

Figure 5.16: Battery final SOC – no cooling.

It is noticed that specific consumption increases. The reason for that is with de-rate strategy the rate of motor torque increase is limited to lower value at the extreme conditions so the distance covered is less. Nevertheless, the final SOC in the end is higher.

- Maximum motor temperature:

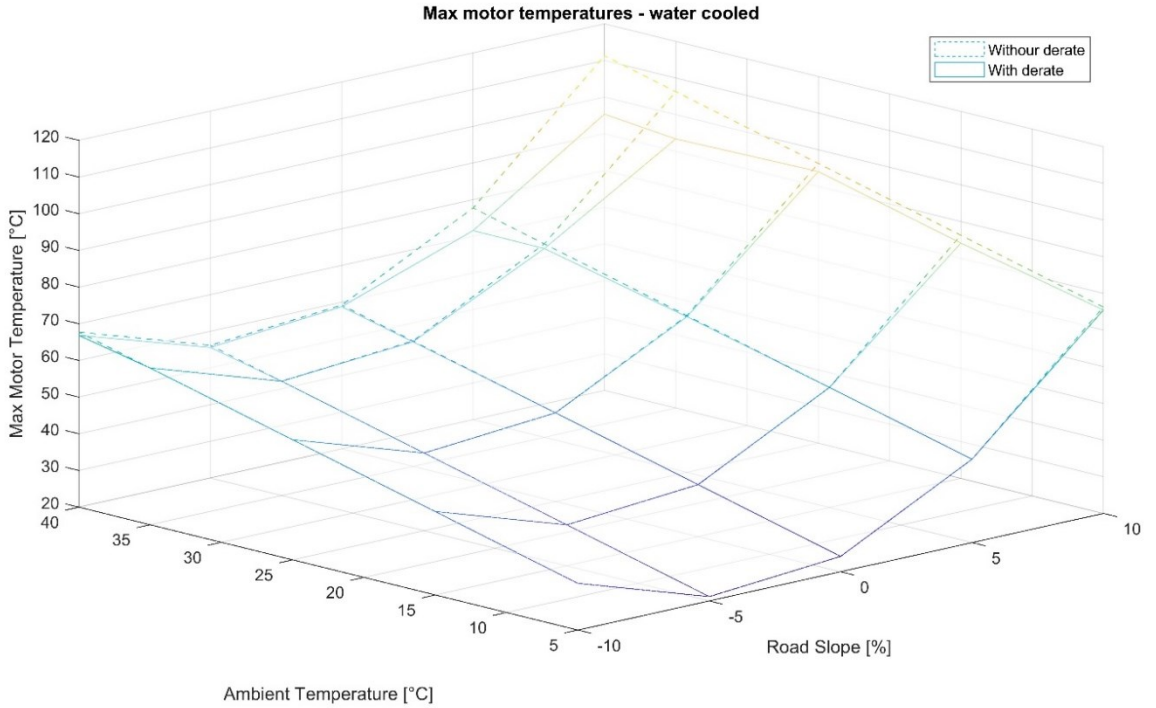

Figure 5.17: Maximum motor temperature – water cooled.

Due to the limitation in motor torque increase rate with de-rate strategy an improvement in maximum motor temperature can be achieved as well. This change in motor maximum temperature does not depend on battery type as motor draws the same current for each torque in any case.

It is important to know the difference between the predicted temperature by the prediction algorithm and the real temperature to know prediction accuracy. This is shown in the following figure.

- Prediction accuracy:

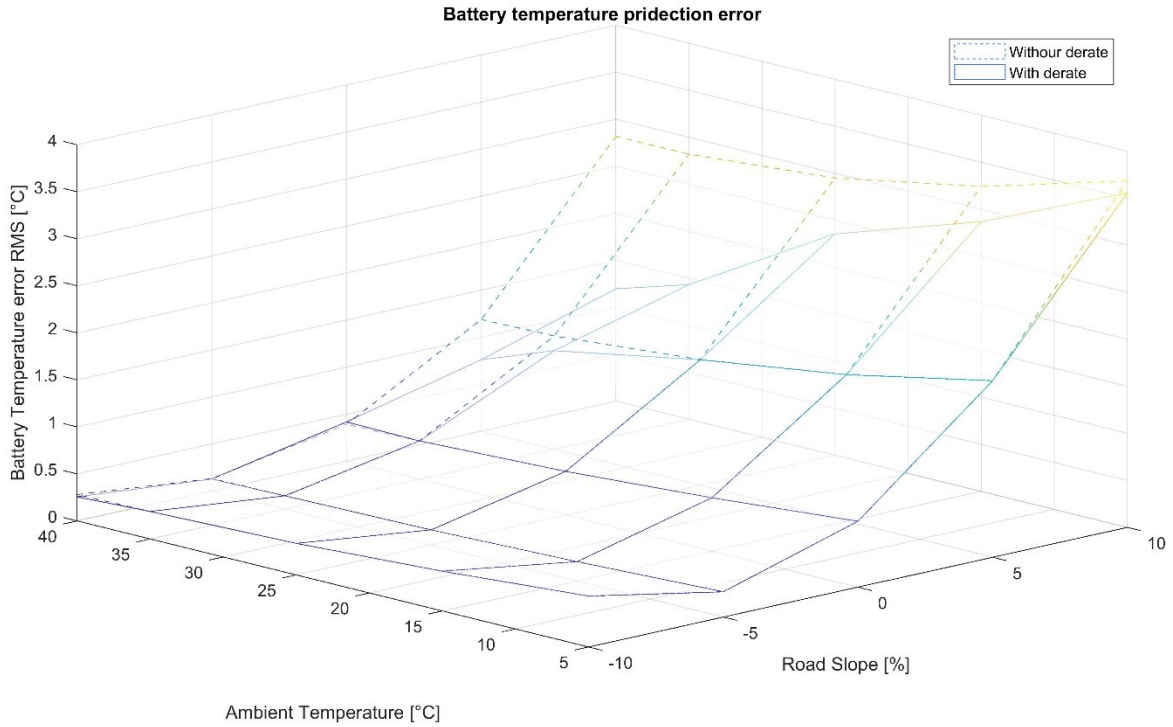

Figure 5.18: Error in battery temperature prediction.

Figure 5.18 shows the difference between actual battery temperature from simulation and the temperature predicted before using prediction algorithm. With de-rate strategy the error in battery temperature prediction is much lower.

Disadvantages (deration cost):

- Velocity profile error:

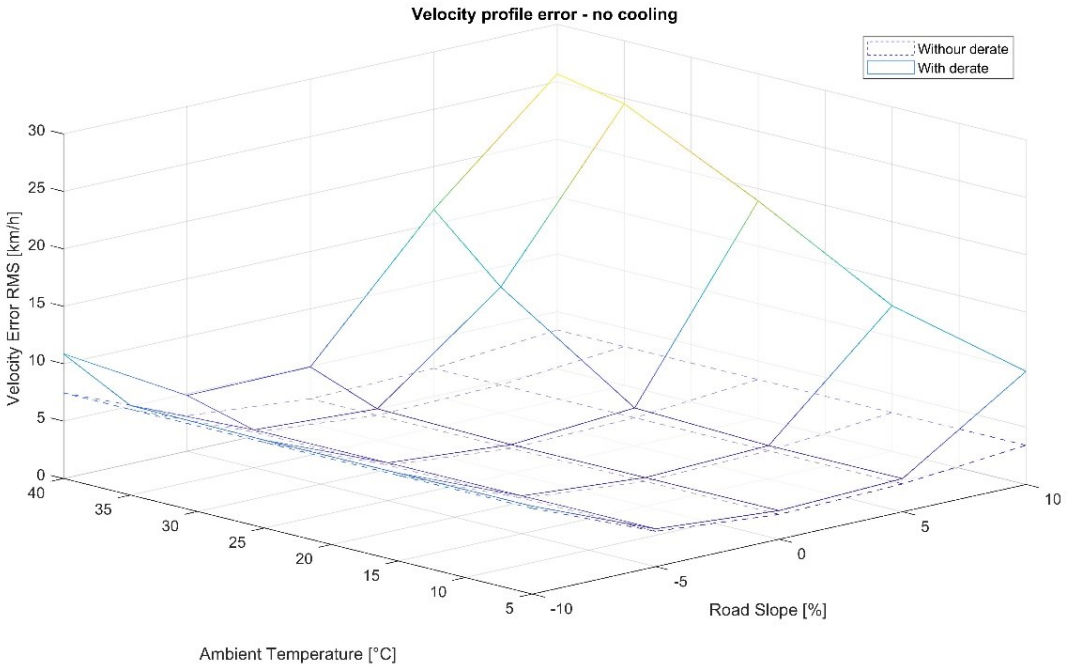

Figure 5.19: Velocity profile error – no cooling.

There is a disadvantage of de-rate strategy it can be noticed in the speed of vehicle response to velocity increase commands. Sometimes especially in extreme conditions when the battery provides higher current and generates more heat there can be a delay in vehicle response to velocity command due to motor torque increase rate limitation. In the end vehicle will reach the commanded velocity but with lower rate to avoid battery overheating. This delay appears in figure 5.19.

5.4.4 Ambient air cooling:

It was seen that the de-rate strategy showed promising results in the absence of cooling. In the following section, the same procedure is repeated with cooling by ambient air forced by vehicle speed. It is expected that de-rate strategy will show even better results.

- Average battery heat generation:

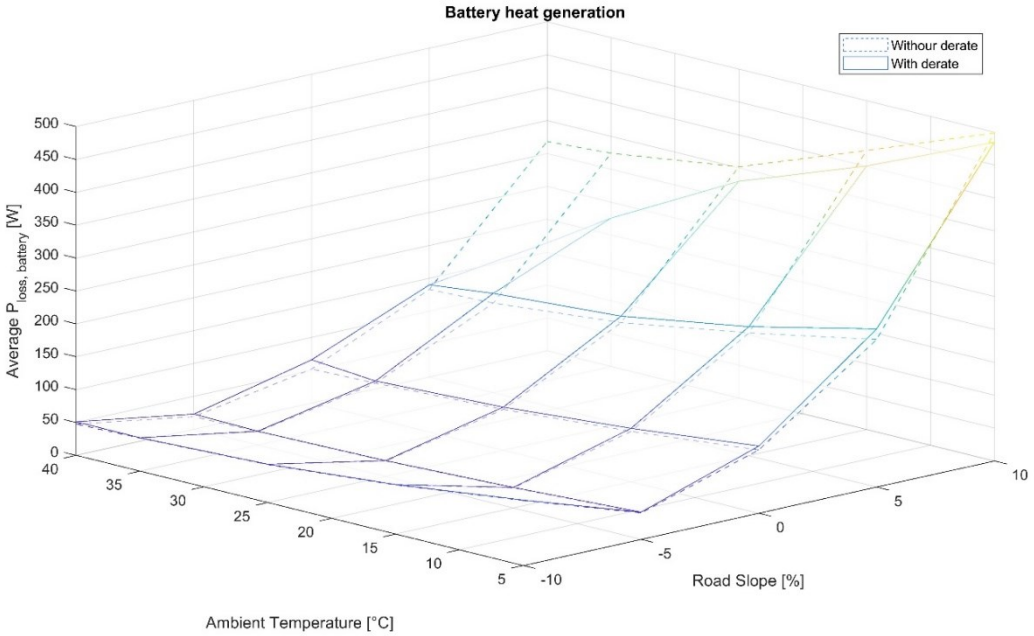

Figure 5.20: Average battery heat generation – ambient air cooling.

There is a slight change in battery heat generation as this quantity depends on the amount of discharge current and this depends on motor torque.

- Cooling power:

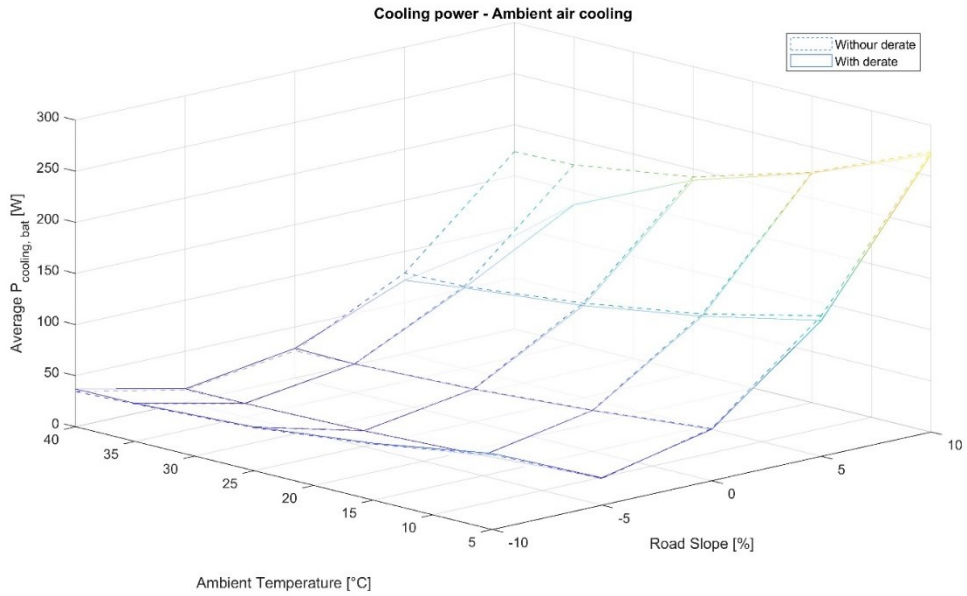

Figure 5.21: Cooling power – ambient air cooling.

- Maximum battery temperature:

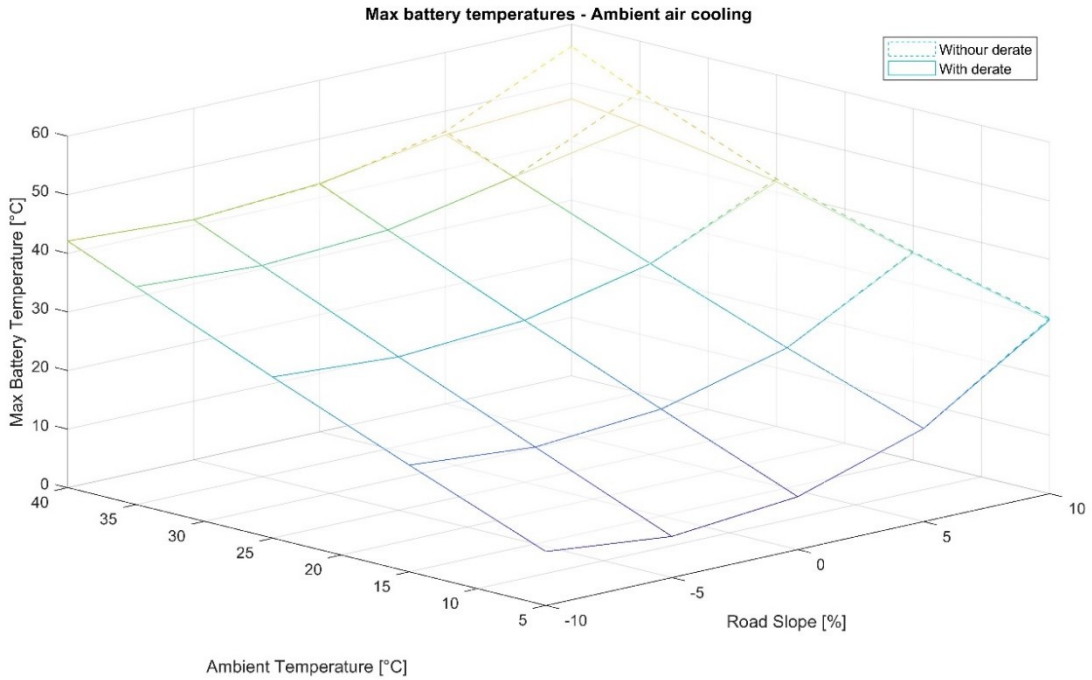

Figure 5.22: Maximum battery temperature – ambient air cooling.

Maximum battery temperature is lower with deration and overheating is completely avoided with only ambient air cooling.

- Battery overheating duration:

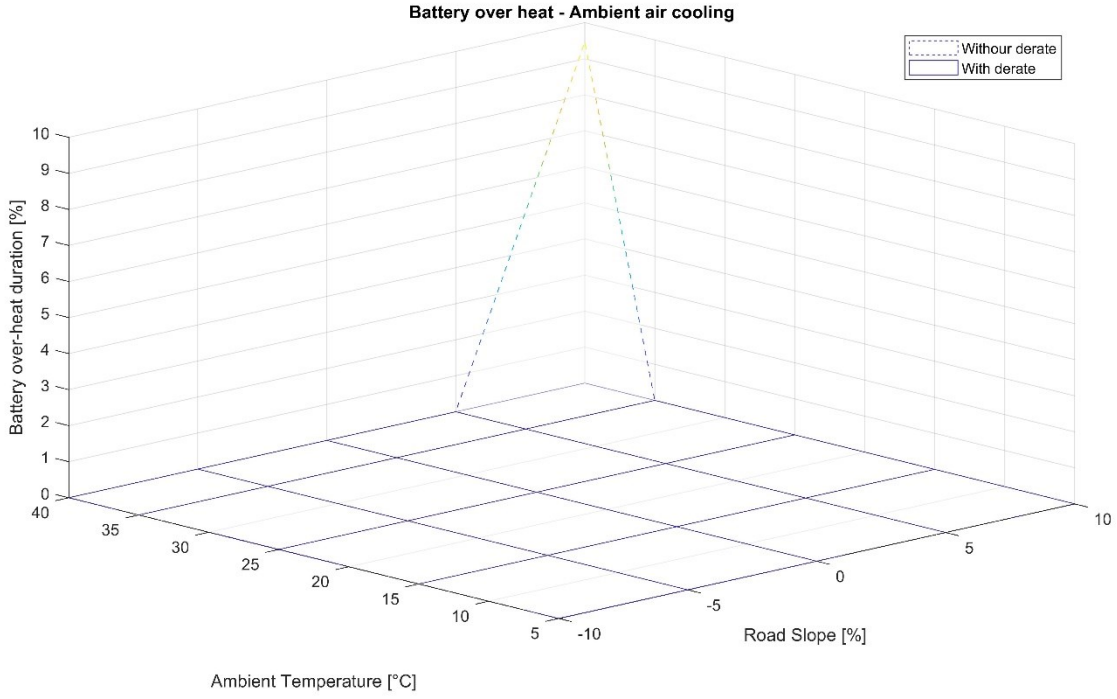

Figure 5.23: Battery overheating duration – ambient air cooling.

- Consumption:

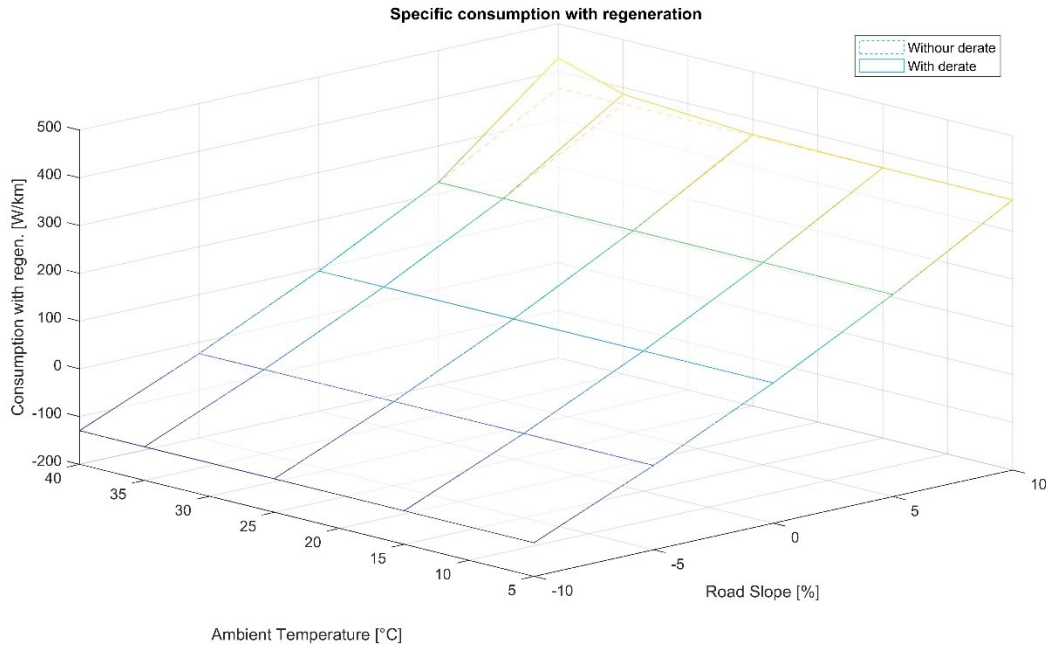

Figure 5.24: Specific consumption with regeneration – ambient air cooling.

- Battery final SOC:

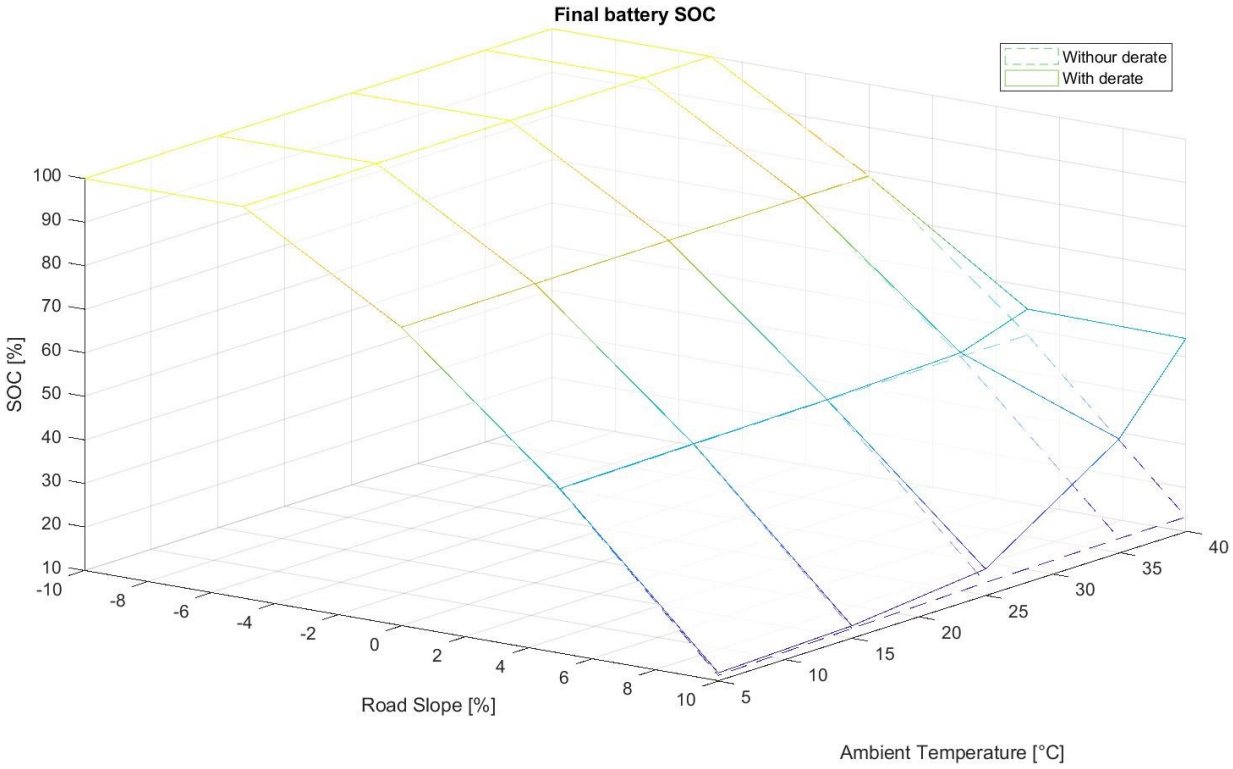

Figure 5.25: Battery final SOC – ambient air cooling.

As stated before specific consumption is a little higher with deration because the distance covered by the vehicle is lower but the final SOC of the battery is higher.

- Prediction accuracy:

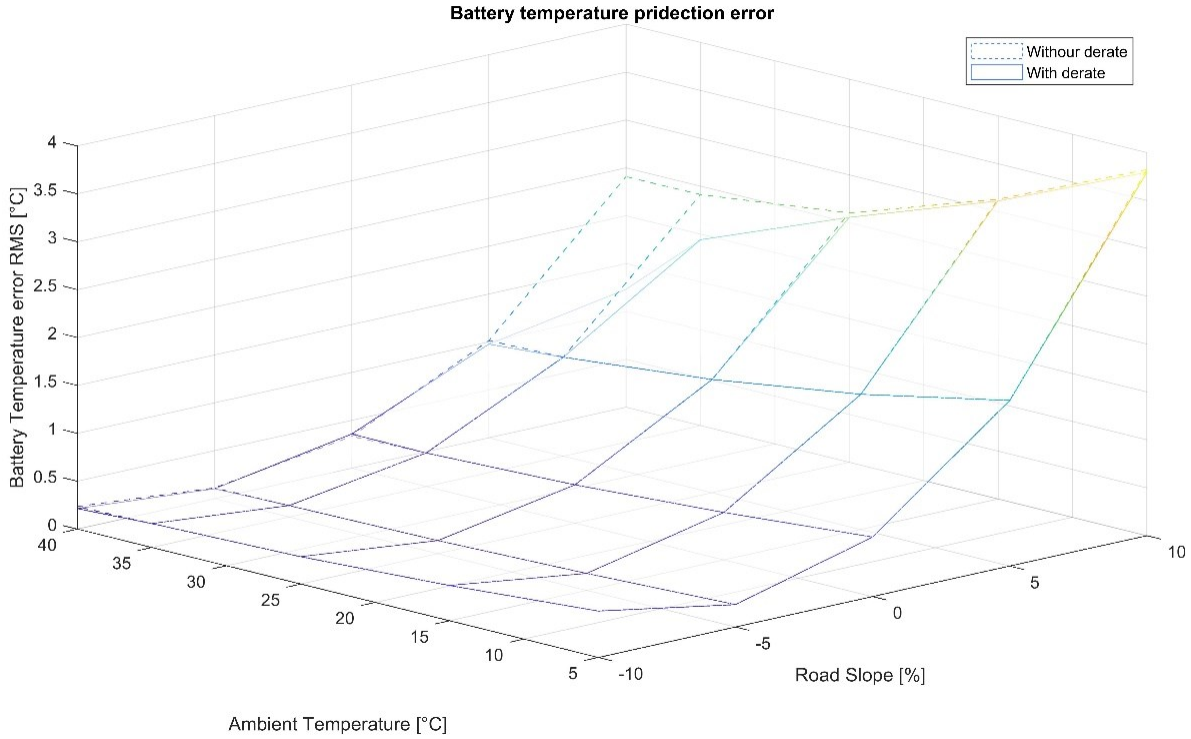

Figure 5.26: Battery temperature prediction error – ambient air cooling.

- Velocity profile error:

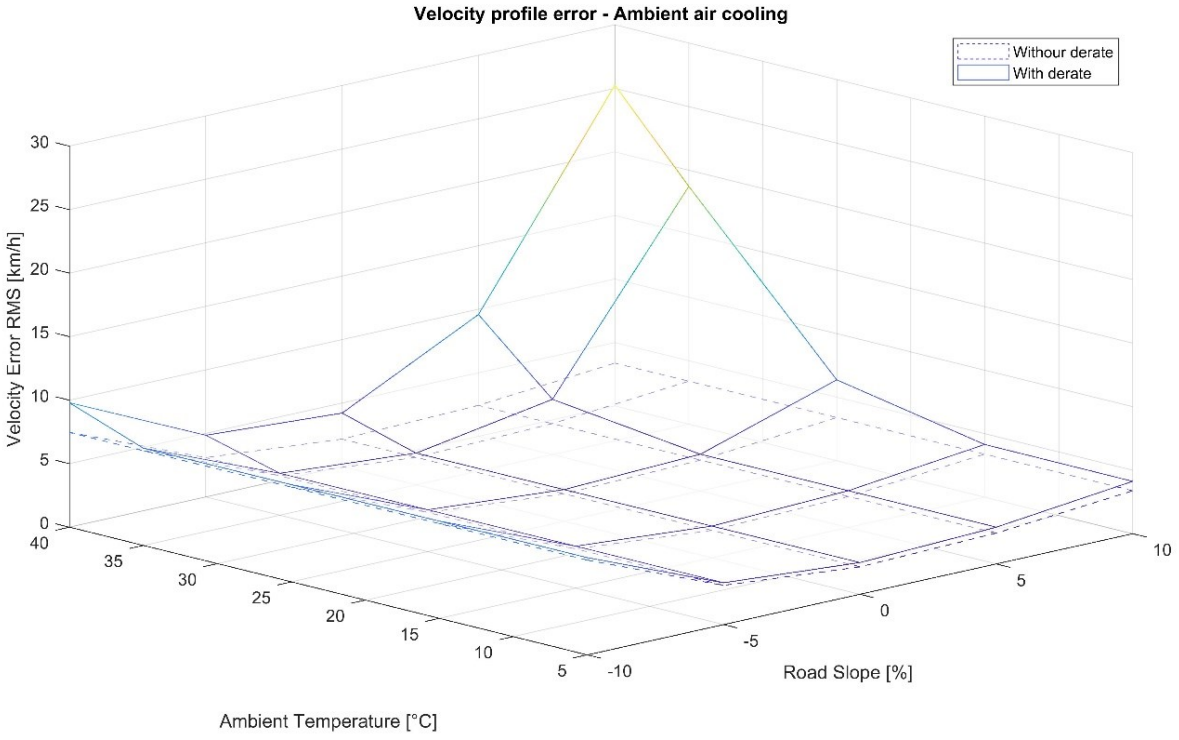

Figure 5.27: Velocity profile error – ambient air cooling.

With cooling the error in velocity profile is less which means the difference between vehicle velocity and the commanded velocity is less. This is because with cooling, battery temperature is lower so it allows higher motor torque increase rate which makes the vehicle more responsive and improves the efficiency of de-rate strategy.

Useful information to assess the effectiveness of the proposed de-rate strategy and cooling system is what driving mode is selected in each case and for how long. Figures 5.28, 5.29 show these results for no cooling and ambient air cooling cases respectively.

- Driving modes lengths:

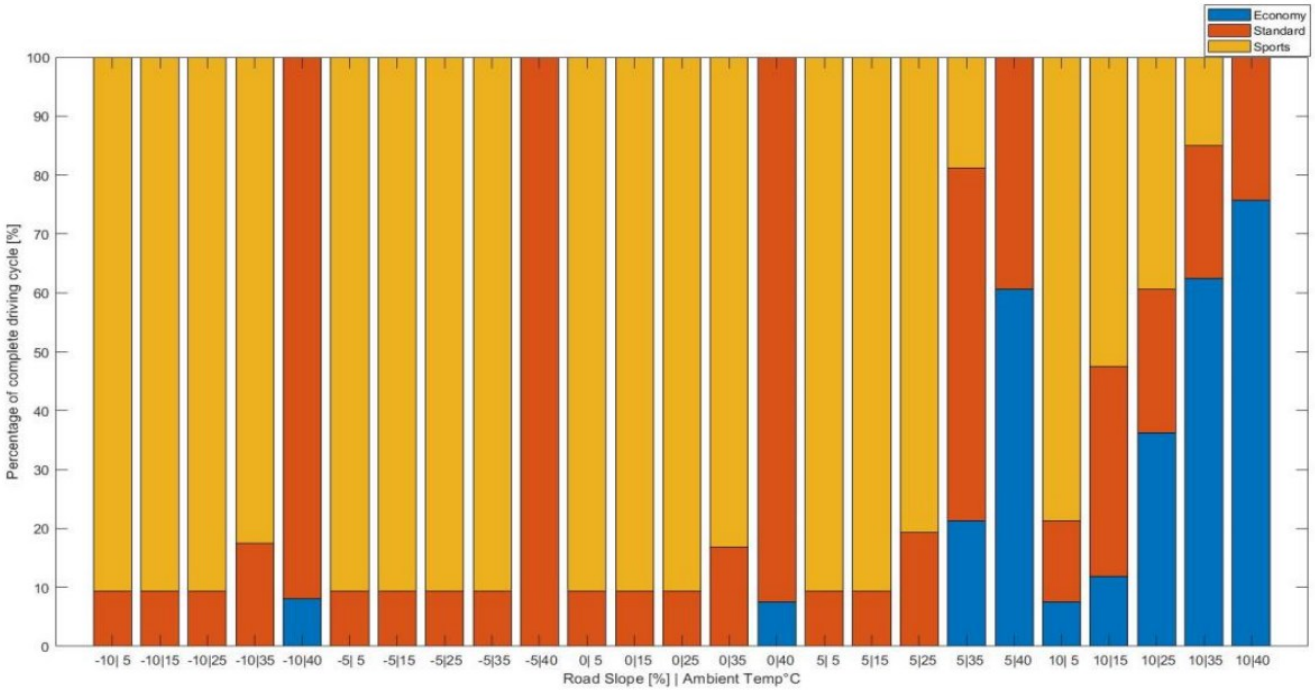

Figure 5.28: Driving modes duration – no cooling.

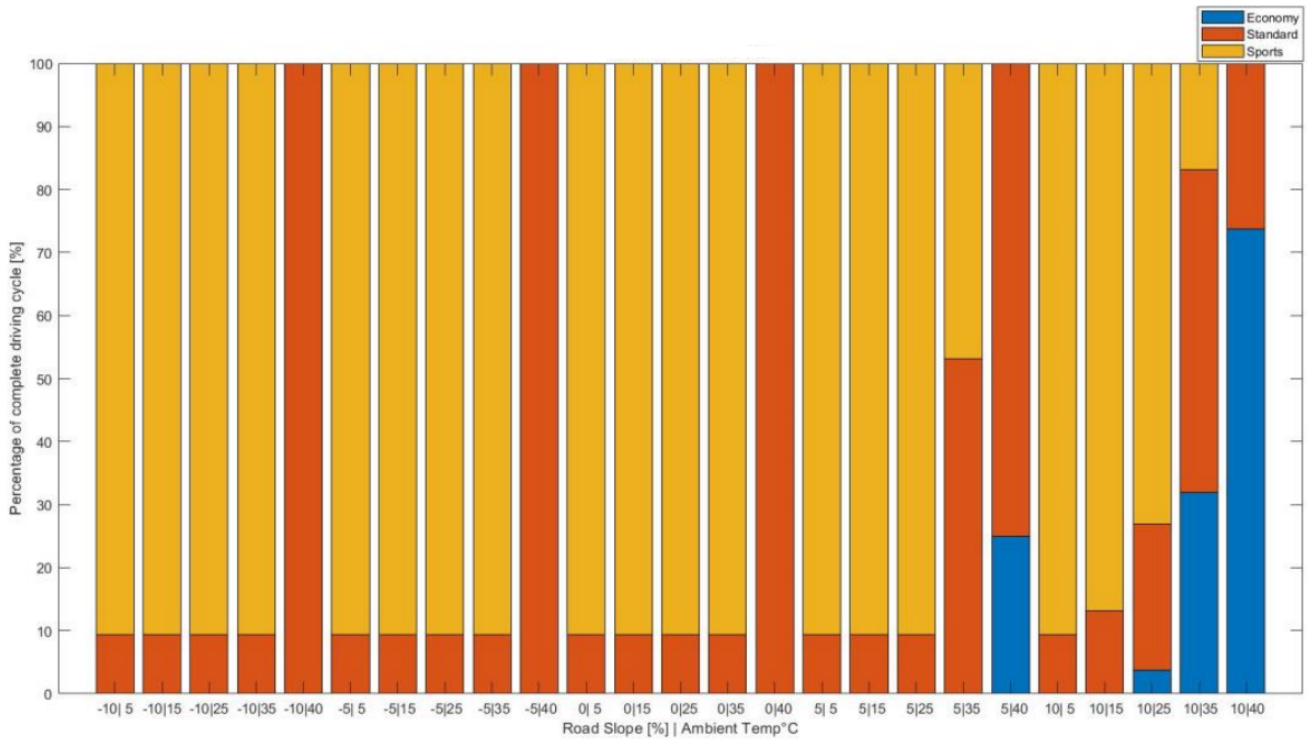

Figure 5.29: Driving modes duration – ambient air cooling.

It should be noted that in all the experiments, the de-rating system begins with Standard mode as its default choice until it reaches the first prediction instance and then a driving mode is selected according to the prediction results. This is why all of the bars include at least a small part of Standard driving mode.

6. CONCLUSION

Covered topics in this thesis:

- Designing battery and cooling system MATLAB Simulink models that are easily modular to any cell type and can be with or without cooling system by a simple selection.
- Comparison between LG cell and Samsung cell.
- Designing a 10 KWh battery pack and studying its performance in some realistic situations, also studying different cooling systems:
    - Ambient air cooling forced my vehicle movement.
    - Cooling by cooled air at 15 ºC and flowing at 3 m/s.
- Prediction of future battery and motor temperatures and exploiting de-rate strategy to overcome overheating problem.

It was found that Samsung battery cells have better performance from thermal point of view and reached lower temperatures than LG cells moreover, Samsung cells have a higher temperature threshold limit. Next, different cooling systems were studied without any deration. Ambient air cooling method by passing cooling air in the tubes in the base of battery packaging box forced by vehicle movement is used. Good results were obtained from the cooling system except for extreme case of road slope 10% and atmospheric temperature 40 ºC. When it came to cooled air cooling system overheating problem was completely eliminated.

Finally, a more complicated algorithm implementing prediction/deration strategy was used to solve the overheating problem. Prediction algorithm that uses data from driver's behavior in the specified time history window to prediction future temperatures of battery and motor. Then a de-rate strategy that limits the maximum motor torque increase rate based on the predicted values is applied. This showed good results and overheating problem was completely eliminated with ambient air cooling system without the need of air conditioning system.

REFERENCES

[1] Z.-Y. She, Qing Sun, J.-J. Ma, and B.-C. Xie, "What are the barriers to widespread adoption of battery electric vehicles? A survey of public perception in Tianjin, China," *Transp. Policy*, vol. 56, pp. 29–40, 2017, doi: https://doi.org/10.1016/j.tranpol.2017.03.001.

[2] "Global EV Outlook 2020," *Glob. EV Outlook 2020*, 2020, doi: 10.1787/d394399e-en.

[3] W. Li, R. Long, and H. Chen, "Consumers' evaluation of national new energy vehicle policy in China: An analysis based on a four paradigm model," *Energy Policy*, vol. 99, pp. 33–41, 2016, doi: https://doi.org/10.1016/j.enpol.2016.09.050.

[4] S. Bubeck, J. Tomaschek, and U. Fahl, "Perspectives of electric mobility: Total cost of ownership of electric vehicles in Germany," *Transp. Policy*, vol. 50, pp. 63–77, 2016, doi: https://doi.org/10.1016/j.tranpol.2016.05.012.

[5] M. A. Hannan, M. S. H. Lipu, A. Hussain, and A. Mohamed, "A review of lithium-ion battery state of charge estimation and management system in electric vehicle applications: Challenges and recommendations," *Renew. Sustain. Energy Rev.*, vol. 78, pp. 834–854, 2017, doi: https://doi.org/10.1016/j.rser.2017.05.001.

[6] D. V Pelegov and J. Pontes, "Main Drivers of Battery Industry Changes: Electric Vehicles—A Market Overview," *Batteries* , vol. 4, no. 4. 2018, doi: 10.3390/batteries4040065.

[7] D. Bresser *et al.*, "Perspectives of automotive battery R&D in China, Germany, Japan, and the USA," *J. Power Sources*, vol. 382, pp. 176–178, 2018, doi: https://doi.org/10.1016/j.jpowsour.2018.02.039.

[8] Y. Ding, Z. P. Cano, A. Yu, J. Lu, and Z. Chen, "Automotive Li-Ion Batteries: Current Status and Future Perspectives," *Electrochem. Energy Rev.*, vol. 2, no. 1, pp. 1–28, 2019, doi: 10.1007/s41918-018-0022-z.

[9] G. A. Nazri and G. Pistoia, *Lithium Batteries: Science and Technology*. Springer US, 2003.

[10] B. Park, C. ho Lee, C. Xia, and C. Jung, "Characterization of gel polymer electrolyte for suppressing deterioration of cathode electrodes of Li ion batteries on high-rate cycling at elevated temperature," *Electrochim. Acta*, vol. 188, pp. 78–84, 2016, doi: https://doi.org/10.1016/j.electacta.2015.11.102.

[11] W. Sung and C. B. Shin, “Electrochemical model of a lithium-ion battery implemented into an automotive battery management system,” *Comput. Chem. Eng.*, vol. 76, pp. 87–97, 2015, doi: https://doi.org/10.1016/j.compchemeng.2015.02.007.

[12] M. A. Rahman, S. Anwar, and A. Izadian, “Electrochemical model parameter identification of a lithium-ion battery using particle swarm optimization method,” *J. Power Sources*, vol. 307, pp. 86–97, 2016, doi: https://doi.org/10.1016/j.jpowsour.2015.12.083.

[13] R. Klein, N. A. Chaturvedi, J. Christensen, J. Ahmed, R. Findeisen, and A. Kojic, “Electrochemical Model Based Observer Design for a Lithium-Ion Battery,” *IEEE Trans. Control Syst. Technol.*, vol. 21, no. 2, pp. 289–301, 2013, doi: 10.1109/TCST.2011.2178604.

[14] C. Zou, C. Manzie, and D. Nešić, “A Framework for Simplification of PDE-Based Lithium-Ion Battery Models,” *IEEE Trans. Control Syst. Technol.*, vol. 24, no. 5, pp. 1594–1609, 2016, doi: 10.1109/TCST.2015.2502899.

[15] P. Moss, G. Au, E. Plichta, and J. Zheng, “An Electrical Circuit for Modeling the Dynamic Response of Li-Ion Polymer Batteries,” *J. Electrochem. Soc.*, vol. 155, pp. A986–A994, Dec. 2008, doi: 10.1149/1.2999375.

[16] X. Hu, S. Li, and H. Peng, “A comparative study of equivalent circuit models for Li-ion batteries,” *J. Power Sources*, vol. 198, pp. 359–367, 2012, doi: https://doi.org/10.1016/j.jpowsour.2011.10.013.

[17] S. Nejad, D. T. Gladwin, and D. A. Stone, “A systematic review of lumped-parameter equivalent circuit models for real-time estimation of lithium-ion battery states,” *J. Power Sources*, vol. 316, pp. 183–196, 2016, doi: https://doi.org/10.1016/j.jpowsour.2016.03.042.

[18] T. Huria, M. Ceraolo, J. Gazzarri, and R. Jackey, “High fidelity electrical model with thermal dependence for characterization and simulation of high power lithium battery cells,” in *2012 IEEE International Electric Vehicle Conference*, 2012, pp. 1–8, doi: 10.1109/IEVC.2012.6183271.

[19] T. L. Bergman, A. S. Lavine, and F. P. Incropera, *Fundamentals of Heat and Mass Transfer, 7th Edition*. John Wiley & Sons, Incorporated, 2011.

[20] Datasheet Battery
https://www.mathworks.com/help/autoblks/ref/datasheetbattery.html

[21] MATLAB Function
https://www.mathworks.com/help/simulink/slref/matlabfunction.html